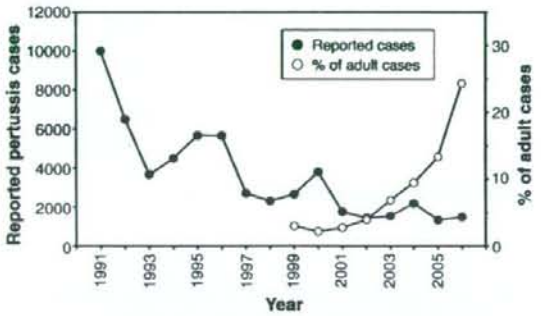

Figure 1 Reported pertussis cases and % of adult cases (≥20 years old) in Japan. The data were obtained from Infectious Disease Surveillance data of the Ministry Health, Labor and Welfare of Japan. The adult cases before 1998 were not monitored.

2002 to the present, although there has been no significant change in the diagnostic method. Based on the Infectious Disease Surveillance data of the Ministry of Health, Labor and Welfare of Japan, the pertussis incidence rates of adults (≥20 years old) were 4.0, 6.9, 9.5, 13.4 and 24.3% of the total reported cases in 2002–2006, respectively (Fig. 1). Although, high attack rates of pertussis have been observed in adults/adolescents even in the high vaccinating countries, it is not clear whether the adult/adolescent pertussis and *B. pertussis* recently circulating strain are associated with each other.

During the last decade, antigenic and genetic divergences in *B. pertussis* circulating strains have been observed in many countries [8–16]. The antigenic variants have been found in the S1 subunit of pertussis toxin (*ptxS1*) and pertactin (*prn*), which are important virulence factors of *B. pertussis*. In the United States, Canada, Russia and European countries, vaccine-types *ptxS1B* and *prn1* alleles of circulating strains have been replaced mainly with nonvaccine-types *ptxS1A* and *prn2*, respectively [8,9,14]. In Japan, the antigenic shifts have been observed from the mid-1990s, and two *ptxS1* (*ptxS1A* and *ptxS1B*) and 4 *prn* (*prn1*, *prn2*, *prn3* and *prn12*) allelic variants have been identified so far [17,18]. The novel variant, *prn12*, was found in one isolate collected in 1991 (GenBank accession no AB278117). Besides the antigenic shifts, the genetic divergence of *B. pertussis* virulence factors, tracheal colonization factor (*tcfA*), filamentous hemagglutinin (*fhaB*) and serotype 2 and 3 fimbriae (*fim2* and *fim3*), has also been found in several countries [13,19–21]. It has been suggested that the shifts in *B. pertussis* recently circulating strains have been induced as a vaccine-driven evolution [9,11]. However, it is unclear whether or not the divergence in the antigenic/virulence-associated proteins is indeed implicated in the increase of the adult/adolescent pertussis patients.

The aims of the present study were (i) to determine the genetic similarity in *B. pertussis* isolates recovered from adults and children by pulsed-field gel electrophoresis (PFGE) analysis, and (ii) to investigate the divergence in the antigenic/virulence-associated allelic variants in the adult strains and to compare this with the child strains. We also wanted to investigate the relationship between the allelic variation and the adult pertussis.

Materials and methods

Isolates

Seven and 53 *B. pertussis* clinical isolates recovered from adults (≥20 years old) and children [0–11 year(s) old], respectively, were investigated in the present study. All of the isolates were collected from nonepidemiologically related cases of pertussis during the period of 1991–2007 in Japan. The number of available adult strains from the laboratory collection of the National Institute of Infectious Diseases (NIID, Japan) was 7 due to the difficulty in isolating the organism from previously immunized persons, whereas the 53 child strains were randomly selected from the laboratory collections so as to reflect the same temporal distribution. Among the adult strains, three (BP173, BP183 and BP313) were recovered from individual familial infection cases, but the clinical associations of the others (BP241, BP239, BP245 and BP316) were unknown (Table 1). The isolates were cultured on Bordet-Gengou agar (Difco) supplemented with 1% glycerol and 15% defibrinated horse blood and incubated at 37 °C for 2–3 days.

PFGE analysis

PFGE was performed on a CHEF Mapper apparatus (Bio-Rad, Hercules, CA, USA) according to standardized recommenda-

Table 1 *Bordetella pertussis* isolates recovered from adults in Japan

Isolate	Isolation year	PFGE type	MLST	Patient		
				Age	Sex	Infection route
BP173	1991	A	MLST-1	32	Female	Household contact
BP183	1991	A	MLST-1	>20[a]	Male	Household contact
BP241	2003	A	MLST-1	27	Male	NA[b]
BP239	2004	B	MLST-2	38	Female	NA
BP245	2004	A	MLST-1	73	Female	NA
BP313	2006	A	MLST-1	58	Female	Household contact
BP316	2007	A	MLST-3	53	Female	NA

[a] Precise age unknown.
[b] Data not available.

tions for typing of *B. pertussis* [22]. The run condition was selected by the autoalgorithm mode of the system with a size range of 20–300 kb. The PFGE patterns were analyzed by the unweighted pair-group method with arithmetic averages (UPGMA) using Diversity Database version 1.1 software (PDI, Inc).

Genotyping

PtxS1 and *prn* of *B. pertussis* isolates were genotyped as described previously [18]. For *fim2*, *fim3* and *tcfA*, the complete open reading frames were sequenced [21]. On the other hand, *fhaB* was sequenced between positions 2250 to 2750, which contains the single polymorphic site identified previously [21]. Sequence reactions were carried out with BigDye terminator v.1 cycle sequencing kit (Applied Biosystems, Foster City, CA), and the products were sequenced on an ABI PRISM 3130xl Genetic Analyzer (Applied Biosystems).

Multilocus sequence typing (MLST)

Among 60 *B. pertussis* isolates tested, allelic variation was observed only in the three genes, *ptxS1*, *prn* and *fim3*. These combined allelic profiles were used to define MLSTs.

Statistic analysis

The chi-square test was employed. A value of $P < 0.05$ was considered to be significant.

Results

Genetic relationship between *B. pertussis* adult and child strains

To investigate the genetic relationship between adult and child strains, their PFGE profiles were analyzed in 7 and 53 clinical isolates recovered from adults and children, respectively. As shown in Fig. 2, 36 PFGE profiles were identified among the adult and child strains, and the profiles were classified into two major groups (type A and B) using UPGMA. The adult strains showed 6 different PFGE profiles, but the strains could be classified into the two groups; 6 isolates (BP173, BP183, BP241, BP245, BP313 and BP316) were type A and 1 isolate (BP239) was type B (Table 1 and Fig. 2). Of the 7 adult strains, 2 isolates (BP183 and BP316) had the same PFGE profile and 3 isolates (BP183, BP313 and BP316) had PFGE profiles to specific adults. However, the phylogenetic analysis of PFGE profiles demonstrated that all of the adult strains were closely related to the child strains (78–100% genetic similarity).

Distribution of antigenic and virulence-associated allelic variants in *B. pertussis* adult and child strains

To identify the antigenic/virulence-associated allelic variants in the adult strains, we carried out sequencing analyses of *ptxS1*, *prn*, *fim2*, *fim3*, *fhaB* and *tcfA* genes. Table 2 shows

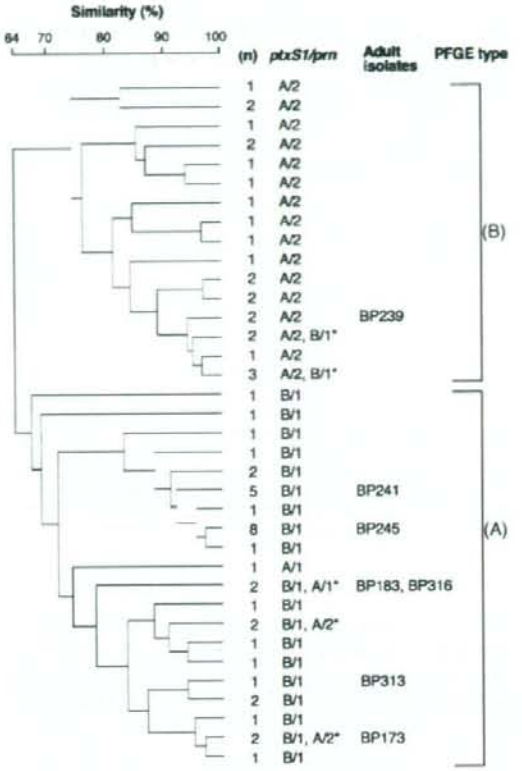

Figure 2 Phylogenetic tree of PFGE profiles of *Bordetella pertussis* isolates recovered from adults and children. The dendrogram was calculated by UPGMA. The adult isolates are indicated by their strain number (BP173, BP183, BP239, BP241, BP245, BP313 and BP316). The regions including the *ptxS1* and *prn* repeat were sequenced, and the combination of *ptxS1* and *prn* alleles is shown as *ptxS1/prn*, e.g., B/1 indicates *ptxS1B/prn1*. * One isolate had different *ptxS1/prn* alleles in the PFGE profile: BP173, B/1; BP183, B/1; BP316, A/1.

the distribution of the antigenic/virulence-associated allelic variants between the adult and child strains. Among the adult strains, *ptxS1B* and *ptxS1A* were detected in 71.4% ($n = 5$) and 28.6% ($n = 2$) of the isolates, respectively, and *prn1* and *prn2* in 85.7% ($n = 6$) and 14.3% ($n = 1$), respectively. For *fim3* gene, only *fim3A* was detected in the adult strains. On the other hand, among the child strains, *ptxS1B* and *ptxS1A* were detected in 54.7% ($n = 29$) and 45.3% ($n = 24$) of the isolates, *prn1* and *prn2* in 56.6% ($n = 30$) and 43.4% ($n = 23$), and *fim3A* and *fim3B* in 84.9% ($n = 45$) and 15.1% ($n = 8$), respectively. The distributions of *ptxS1*, *prn* and *fim3* alleles between the adult and child strains were not statistically significant ($P = 0.42$, 0.14, and 0.27, respectively), although the number of adult strains was somewhat low for meaningful analysis. Interestingly, *fim3B* was first observed in 1994 in Canada and then in Taiwan and Russia [8,19,20], whereas the variant was first identified from 2004 in Japan.

Table 2 Comparison of *Bordetella pertussis* antigenic and virulence-associated allelic variants between adult strains and child strains

Gene	Allele	Type[a]	% Frequency (*n*)	
			Adult strain (*n* = 7)	Child strain (*n* = 53)
ptxS1	*ptxS1B*	Vaccine	71.4 (5)	54.7 (29)
	ptxS1A	Nonvaccine	28.6 (2)	45.3 (24)
prn	*prn1*	Vaccine	85.7 (6)	56.6 (30)
	prn2	Nonvaccine	14.3 (1)	43.4 (23)
fim2	*fim2-1*	Vaccine	100 (7)	100 (53)
fim3	*fim3A*	Vaccine	100 (7)	84.9 (45)
	fim3B	Nonvaccine		15.1 (8)
fhaB	*fhaB1*	Vaccine	100 (7)	100 (53)
tcfA	*tcfA2*	Vaccine	100 (7)	100 (53)

[a] The Japanese vaccine strain Tohama harbors *ptxS1B*, *prn1*, *fim2-1*, *fim3A*, *fhaB1* and *tcfA2* alleles.

For *fim2*, *fhaB* and *tcfA* genes, each variant (*fim2-1*, *fhaB1* and *tcfA2*) was identified among the adult and child strains. There was no allelic variation in *fim3*, *fhaB* and *tcfA*. The Japanese vaccine strain Tohama harbored *ptxS1B*, *prn1*, *fim2-1*, *fim3A*, *fhaB1* and *tcfA2* alleles.

MLSTs of *B. pertussis* adult and child strains

Three genes (*ptxS1*, *prn* and *fim3*) were used to define MLSTs. Among 60 *B. pertussis* isolates tested, five MLSTs (MLST-1 to -5) were identified by the combined allelic profiles (Table 3). Three (MLST-1 to -3) and 5 MLSTs (MLST-1 to -5) were found in the adult and child strains, respectively. MLST-1 was predominant in both strains. Five (71.4%) of 7 adult strains and 25 (47.2%) of 53 child strains were MLST-1, respectively. Among the adult strains, MLST-1 strains were found from 1991 to 2006, and MLST-2 and MLST-3 in 2004 and 2007, respectively (Table 1). The differences in frequencies of the MLSTs between adult and child strains were not statistically significant ($P = 0.28$). The Japanese vaccine strain Tohama was MLST-1.

Discussion

In the present study, we demonstrated that (i) PFGE profiles of adult strains were closely related to those of child strains (78–100% genetic similarity), and (ii) there were no significant differences in the distribution of the antigenic/virulence-associated allelic variants between the adult and child strains. These results indicate that *B. pertussis* adult strains are indistinguishable from the child strains by molecular typing methods. To estimate the possibility of acquisition of novel virulence factor(s) in adult strains, we also performed a comparative proteomic analysis of the adult and child strains. However, no apparent difference was observed in their protein profiles (data not shown). Our observations strongly suggest that there is no *B. pertussis* circulating strain specific to adults, and that the circulating strains have an ability to infect not only children but also adults.

Previously, De Schutter et al. [23] reported that Belgian *B. pertussis* adult strains, recovered from familial infections in the period of 1999–2002, harbored nonvaccine-types *ptxS1A* and *prn2* (or *prn3*) alleles. However, in European countries and the United States, the genetic shifts observed in *ptxS1* and *prn* alleles had already occurred since the 1990s [8,9,14]. The most circulating strains therefore harbored *ptxS1A* and *prn2* (or *prn3*) alleles in those countries. In contrast, approximately half of the Japanese circulating strains, collected in the period of 1991–2007, harbored vaccine-types *ptxS1B* and *prn1* alleles, indicating that the shifts have now progressed in Japan (this study). Therefore, the present study showed the actual relationship between the antigenic shift and *B. pertussis* adult strains, i.e., there was no apparent antigenic shift in the adult strains. In a previous report, Mastrantonio et al. [24] demonstrated that the frequency of vaccine-type *prn1* allele in strains recovered from unvaccinated children was higher than that of vaccinated children. They suggested that *B. pertussis* strains harboring *prn1* allele might be more affected by vaccine-induced immunity than the strains harboring nonvaccine-type *prn2* or *prn3* allele. However, in the present study, no such difference in the distribution of *prn* allelic variants was observed between adult and child strains.

In Japan, the acellular pertussis vaccines introduced in 1981 have successfully controlled pertussis in children. However, the incidence of reported pertussis cases of adults has considerably increased from 2002 to the present. The waning of vaccine-acquired immunity and decreased oppor-

Table 3 MLST frequencies between *Bordetella pertussis* adult strains and child strains

MLST	Alleles	Type[a]	% Frequency (*n*)	
			Adult strain (*n* = 7)	Child strain (*n* = 53)
MLST-1	*ptxS1B/prn1/fim3A*	Vaccine	71.4 (5)	47.2 (25)
MLST-2	*ptxS1A/prn2/fim3A*		14.3 (1)	35.8 (19)
MLST-3	*ptxS1A/prn1/fim3A*		14.3 (1)	1.9 (1)
MLST-4	*ptxS1A/prn2/fim3B*			7.5 (4)
MLST-5	*ptxS1B/prn1/fim3B*			7.5 (4)

[a] The Japanese vaccine strain Tohama is MLST-1.

tunities for boosting of immunity because of reduced levels of circulation of *B. pertussis* have been proposed as possible reasons for adult/adolescent pertussis [25]. However, the Japanese adult pertussis cannot be thus explained, since U.S. adult/adolescent pertussis has steadily increased during the last two decades [2–4]. The reason for the rising pertussis incidence in Japanese adult population has remained unclear. Further analyses are warranted to determine the cause of the adult pertussis.

In conclusion, *B. pertussis* isolates recovered from Japanese adults and children were indistinguishable by molecular typing methods. In Japan, the antigenic and genetic shifts, especially *ptxS1* and *prn* alleles, would be unrelated to the rise of the adult pertussis incidence.

Acknowledgements

This work was supported by grants (H18-Shinkou-1 and H19-Shinkou-1) from the Ministry of Health, Labor and Welfare of Japan.

References

[1] Mattoo S, Cherry JD. Molecular pathogenesis, epidemiology, and clinical manifestations of respiratory infections due to *Bordetella pertussis* and other *Bordetella* subspecies. Clin Microbiol Rev 2005;18:326–82.

[2] Cherry JD. The science and fiction of the "resurgence" of pertussis. Pediatrics 2003;112:405–6.

[3] Güris D, Strebel PM, Bardenheier B, Brennan M, Tachdjian R, Finch E, et al. Changing epidemiology of pertussis in the United States: increasing reported incidence among adolescents and adult, 1990–1996. Clin Infect Dis 1999;28:1230–7.

[4] Kretsinger K, Broder KR, Cortese MM, Joyce MP, Ortega-Sanchez I, Lee GM, et al. Preventing tetanus, diphtheria, and pertussis among adults: use of tetanus toxoid, reduced diphtheria toxoid and acellular pertussis vaccine. MMWR Recomm Rep 2006;55(RR–17):1–37.

[5] Cortese MM, Baughman AL, Brown K, Srivastava P. A "new age" in pertussis prevention new opportunities through adult vaccination. Am J Prev Med 2007;32:177–85.

[6] Hewlett EL, Edwards KM. Pertussis–not just for kids. N Engl J Med 2005;352:1215–22.

[7] von König CHW, Halperin S, Riffelmann M, Guiso N. Pertussis of adults and infants. Lancet Infect Dis 2002;2:744–50.

[8] Borisova O, Kombarova SY, Zakharova NS, van Gent M, Aleshkin VA, Mazurova I, et al. Antigenic divergence between *Bordetella pertussis* clinical isolates from the Moscow, Russia, and vaccine strains. Clin Vaccine Immunol 2007;14:234–8.

[9] Cassiday P, Sanden G, Heuvelman K, Mooi F, Bisgard KM, Popovic T. Polymorphism in *Bordetella pertussis* pertactin and pertussis toxin virulence factors in the United States, 1935–1999. J Infect Dis 2000;182:1402–8.

[10] Elomaa A, Advani A, Donnelly D, Antila M, Mertsola J, He Q, et al. Population dynamics of *Bordetella pertussis* in Finland and Sweden, neighbouring countries with different vaccination histories. Vaccine 2007;25:918–26.

[11] Mooi FR, van Oirschot H, Heuvelman K, van der Heide HG, Gaastra W, Willems RJ. Polymorphism in the *Bordetella pertussis* virulence factors P.69/pertactin and pertussis toxin in The Netherlands: temporal trends and evidence for vaccine-driven evolution. Infect Immun 1998;66:670–5.

[12] Mooi FR, He Q, van Oirschot H, Mertsola J. Variation in the *Bordetella pertussis* virulence factors pertussis toxin and pertactin in vaccine strains and clinical isolates in Finland. Infect Immun 1999;67:3133–4.

[13] Packard ER, Parton R, Coote JG, Fry NK. Sequence variation and conservation in virulence-related genes of *Bordetella pertussis* isolates from the UK. J Med Microbiol 2004;53:355–65.

[14] van Amersfoorth SCM, Schouls LM, van der Heide HGJ, Advani A, Hallander HO, Bondeson K, et al. Analysis of *Bordetella pertussis* populations in European countries with different vaccination policies. J Clin Microbiol 2005;43:2834–43.

[15] Weber C, Boursaux-Eude C, Coralie G, Caro V, Guiso N. Polymorphism of *Bordetella pertussis* isolates circulating for the last 10 years in France, where a single effective whole-cell vaccine has been used for more than 30 years. J Clin Microbiol 2001;39:4396–403.

[16] Yao S-M, Lin Y-C, Chou C-Y, Chen Y-Y, Hsiao M-J, Chen H-Y, et al. Antigenic divergence of *Bordetella pertussis* isolates in Taiwan. J Clin Microbiol 2005;43:5457–61.

[17] Guiso N, Boursaux-Eude C, Weber C, Hausman SZ, Sato H, Iwaki M, et al. Analysis of *Bordetella pertussis* isolates collected in Japan before and after introduction of acellular pertussis vaccine. Vaccine 2001;19:3248–52.

[18] Kodama A, Kamachi K, Horiuchi Y, Konda T, Arakawa Y. Antigenic divergence suggested by correlation between antigenic variation and pulsed-field gel electrophoresis profiles of *Bordetella pertussis* isolates in Japan. J Clin Microbiol 2004;42:5453–7.

[19] Lin Y-C, Yao S-M, Yan J-J, Chen Y-Y, Hsiao M-J, Chou C-Y, et al. Molecular epidemiology of *Bordetella pertussis* in Taiwan, 1993–2004: suggests one possible explanation for the outbreak of pertussis in 1997. Microbes Infect 2006;8:2082–7.

[20] Tsang RSW, Lau AKH, Sill ML, Halperin SA, Caeseele PV, Jamieson F, et al. Polymorphisms of the fimbria *fim3* gene of *Bordetella pertussis* strains isolated in Canada. J Clin Microbiol 2004;42:5364–7.

[21] van Loo IHM, Heuvelman KJ, King AJ, Mooi FR. Multilocus sequence typing of *Bordetella pertussis* based on surface protein genes. J Clin Microbiol 2002;40:1994–2001.

[22] Mooi FR, Hallander H, von König CHW, Hoet B, Guiso N. Epidemiological typing of *Bordetella pertussis* isolates: recommendations for a standard methodology. Eur J Clin Microbiol Infect Dis J 2000;19:174–81.

[23] De Schutter I, Malfroot A, Dab I, Hoebrekx N, Muyldermans G, Piérard D, et al. Molecular typing of *Bordetella pertussis* isolates recovered from Belgian children and their household members. Clin Infect Dis 2003;36:1391–6.

[24] Mastrantonio P, Spigaglia P, van Oirschot H, van der Heide HGJ, Heuvelman K, Stefanelli P, et al. Antigenic variants in *Bordetella pertussis* strains isolated from vaccinated and unvaccinated children. Microbiology 1999;145:2069–75.

[25] Wendelboe AM, Van Rie A, Salmaso S, Englund JA. Duration of immunity against pertussis after natural infection and vaccination. Pediatr Infect Dis J 2005;24:S58–61.

JOURNAL OF BACTERIOLOGY, Dec. 2008, p. 7739–7753 Vol. 190, No. 23
0021-9193/08/$08.00+0 doi:10.1128/JB.00361-08

Genetic Analysis of the *Enterococcus* Vancomycin Resistance Conjugative Plasmid pHTβ: Identification of the Region Involved in Cell Aggregation and *traB*, a Key Regulator Gene for Plasmid Transfer and Cell Aggregation▽†

Haruyoshi Tomita[1]* and Yasuyoshi Ike[1,2]

Department of Bacteriology, Gunma University Graduate School of Medicine, Maebashi, Gunma 371-8511, Japan,[1] and Laboratory of Bacterial Drug Resistance, Gunma University Graduates School of Medicine, Maebashi, Gunma 371-8511, Japan[2]

Received 12 March 2008/Accepted 22 September 2008

The *Enterococcus* plasmid pHTβ (63.7 kbp) is a pheromone-independent, highly conjugative pMG1-like plasmid that carries a Tn*1546*-like transposon encoding vancomycin resistance. The transfer-related regions (Tra I, Tra II, and Tra III) containing *oriT* and a putative nickase gene (*traI*) have previously been identified in pHTβ, and in this study, we found that the plasmid conferred the ability to self-aggregate on the host strain *Enterococcus faecalis* FA2-2. A region where mutation resulted in the impairment of aggregation was identified and mapped to a point upstream of the transfer-related Tra I region. This region consisted of an approximately 6-kbp segment that contained the five open reading frames (ORFs) ORF9 to ORF13. These ORFs are considered to encode the aggregation function, although the precise mode of action of each ORF has not yet been elucidated. An in-frame deletion mutant of ORF10 resulted in reduced aggregation and decreased transfer frequency in broth mating. Transcription analysis of the aggregation region showed that the five ORFs from ORF9 to ORF13 form an operon structure, and a long transcript that started from a promoter region located upstream of ORF9 was identified. Tra II spans a 1.7-kbp region containing ORF56 and ORF57. Tn*917-lac* insertions into or an in-frame deletion mutant of ORF56 (187 amino acids) resulted in impaired transfer and aggregation. The cloned ORF56 complemented these functions in *trans*. The transcription levels of ORF10 and ORF13 were reduced in the in-frame mutants of ORF56, but this reduction was complemented by a cloned ORF56 in *trans*. The results indicated that ORF56 positively regulated the aggregation and plasmid transfer in the host strain, and ORF56 was designated *traB*.

The genes and systems required for bacterial conjugation have been classified into two functional groups: the DNA transfer and replication system and the mating pair formation (Mpf) system (24, 40). The DNA transfer and replication system is also referred to as the relaxosome system and is involved in the multiprotein-plasmid DNA complex that is generated at the plasmid origin of transfer (*oriT*) and the generation of the single strand to be transferred to the recipient cell (40).

The Mpf system is a plasmid-encoded multiprotein structure that is involved in the protein complex that establishes intimate contact between donor and recipient, such as the sex pili in gram-negative bacteria, and the formation of the transmembrane channel for the donor plasmid DNA strand to move from donor to recipient cell. The Mpf system is linked with a coupling protein, such as those encoded by *traD* of the F plasmid, *traG* of RP4, and *virD4* of pTi, to deliver the protein-DNA complex generated by the relaxosome system to the entrance of the Mpf channel. A macromolecular transfer system present in gram-negative bacteria that is similar to the conjugal Mpf system has been classified as a type IV secretion system (24).

The nucleotide sequence data for the *tra* region of the gram-positive bacterial conjugative plasmid show homologies with certain protein components of type IV secretion systems (14), and an Mpf system corresponding to the type IV secretion system has recently been identified in the conjugative plasmid pIP501 isolated from gram-positive bacteria (1). The conjugation systems in gram-negative and gram-positive bacteria differ mainly in the mechanisms by which the intimate contact between donor and recipient cell that is a prerequisite for the initiation of conjugative transfer is established. In gram-negative bacteria, this initial contact between donor and recipient cells is mediated by the sex pili. In the majority of gram-positive bacteria, the mechanisms by which the initial cell-to-cell contact is established have not been identified.

Two types of highly efficient conjugative plasmids that are effectively transferred in broth mating have been identified in the gram-positive enterococci (4). One is the pheromone-responsive plasmid found in *Enterococcus faecalis*, and the other is the non-pheromone-responsive plasmid found in *Enterococcus faecium* strains. The pheromone-responsive conjugative plasmids of *E. faecalis* have a unique conjugative system that is the best example of the mechanism of initial cell-to-cell contact in gram-positive bacteria to be elucidated to date. The regulatory process is highly unusual among gram-positive bacteria and is instrumental in the conjugative transfer of the phero-

* Corresponding author. Mailing address: Department of Bacteriology, Gunma University Graduate School of Medicine, Maebashi, Gunma 371-8511, Japan. Phone: (81) 27 220 7992. Fax: (81) 27 220 7996. E-mail: tomitaha@med.gunma-u.ac.jp.

† Supplemental material for this article may be found at http://jb.asm.org/.

▽ Published ahead of print on 3 October 2008.

mone-responsive plasmid. A donor cell harboring a sex pheromone-responsive plasmid responds to the pheromone specific for the plasmid, which generally consists of seven or eight amino acids and is secreted from a potential recipient cell (3, 4, 6). The sex pheromone signal induces synthesis of a surface aggregation substance (AS) that facilitates formation of the mating aggregate (6). The sex pheromone also activates the genes required for plasmid transfer (3, 4). The pheromone (in a culture filtrate of a plasmid-free strain) induces self-aggregation of donor cells and makes donor cells ready for conjugation without mating with recipient cells.

We have previously isolated the pheromone-independent gentamicin resistance conjugative plasmid pMG1 (65.1 kbp) from a gentamicin-resistant *E. faecium* clinical strain in Japan, and this was the first report describing an efficient plasmid transfer system in *E. faecium* (17). pMG1 transfers efficiently from *E. faecium* to *E. faecalis* strains and vice versa and also among different enterococcus species during broth mating at a frequency of about 10^{-4} per donor strain. Southern hybridization analysis did not show any homology to the pheromone-responsive plasmids or to the broad-host-range plasmids pAMβ1 and pIP501, which were originally isolated from *E. faecalis* (18) and *Streptococcus agalactiae* (1), respectively, and transferred on a solid surface at a relatively low frequency. These results indicate that pMG1 is a new type of conjugative plasmid and that another type of efficient broth mating transfer system must be present in *E. faecium* that differs from the sex pheromone-mediated transfer system found in *E. faecalis*. Our epidemiological study revealed that pMG1-like plasmids are widely disseminated in vancomycin-resistant *E. faecium* clinical isolates obtained from a hospital in the United States, suggesting that pMG1-like plasmids may contribute to the efficient dissemination of vancomycin resistance in enterococcus strains (33).

pMG1-like vancomycin resistance pHT plasmids have been isolated from clinical *Enterococcus faecium* and *Enterococcus avium* strains in Japan (34). pHT plasmids, including pHTα (65.9 kbp), pHTβ (63.7 kbp), and pHTγ (66.5 kbp), are highly conjugative plasmids carrying Tn*1546*-like transposons (2) that encode vancomycin resistance (VanA). DNA hybridization shows that the pHT plasmids are related to the conjugative plasmid pMG1, implying that they contain the same efficient conjugation system. pHTβ is the prototype plasmid, and the pHTα and pHTγ plasmids are derivatives of an insertion into pHTβ of an IS*232*-like (2.2-kbp) element and a group II intron (2.8 kbp), respectively. The complete nucleotide sequence of the pHTβ plasmid was determined with the exception of the Tn*1546*-like insertion (10,851 bp). In a previous study, we identified three transfer-related regions within the pHTβ plasmid by genetic analysis using Tn*917-lac* insertion mutagenesis (32). The 39.3-kbp Tra I region is the largest continuous region to be identified. It lies between 2.8 kbp and 42.1 kbp of the plasmid map and contains 46 open reading frames (ORFs) from ORF3 to ORF48. It contains several genes homologous to the reported transfer-related genes of conjugative plasmids and certain components of the type IV secretion system. The Tra II and Tra III regions are physically separated from the Tra I region and are relatively small regions compared to Tra I. Tra II spans a length of 1.7 kbp located between 47.0 kbp and 48.7 kbp of the plasmid map and contains ORF56 and ORF57 (*traA*) (26, 32). The Tra III region consists of ORF61 located between 52.0 kbp and 52.4 kbp of the plasmid map. A novel type of *oriT* region and a putative relaxase/nickase gene designated *traI* (ORF34) have been identified. The *oriT* region resides in a noncoding region (192 bp) lying between ORF31 and ORF32 and contains three direct repeat sequences and two inverted repeat sequences. The putative pHT relaxase (TraI) has been classified as a new member of the MOB_{MG} family (9, 32). Our study of the pHT plasmids showed that *E. faecalis* strains containing the pHTβ plasmid produced cell aggregates, although aggregation was much weaker than the pheromone-induced cell aggregation encoded by the pheromone-responsive plasmids.

In this report, we show that the pHTβ plasmid conferred the cell aggregation property on the host *E. faecalis* strain and we describe the identification of the cell aggregation determinants and the key regulator gene *traB*, which is involved in aggregation and plasmid transfer.

MATERIALS AND METHODS

Bacterial strains, plasmids, oligonucleotides, media, and reagents. The bacterial strains, plasmids, and oligonucleotides used in this study are listed in Table 1 and Table 2. The *Escherichia coli* strain was grown in Luria-Bertani (LB) broth medium (Difco Laboratories) at 37°C. *E. faecalis* strains were grown in Todd-Hewitt broth (THB) (Difco Laboratories) at 37°C. The following antibiotics at the indicated concentrations were used for selection of *E. faecalis*: erythromycin, 12.5 μg ml^{-1}; streptomycin, 250 μg ml^{-1}; kanamycin, 250 μg ml^{-1}; spectinomycin, 250 μg ml^{-1}; chloramphenicol, 20 μg ml^{-1}; rifampin, 25 μg ml^{-1}; and fusidic acid, 25 μg ml^{-1}. Antibiotic concentrations for selection of *E. coli* were as follows: ampicillin, 100 μg ml^{-1}; kanamycin, 40 μg ml^{-1}; chloramphenicol, 50 μg ml^{-1}; and spectinomycin, 50 μg ml^{-1}. All antibiotics were obtained from Sigma Chemical Co. X-Gal (5-bromo-4-chloro-3-indolyl-β-D-galactopyranoside) was used at 40 μg ml^{-1}.

Plasmid/DNA methodology. Recombinant DNA techniques, analyses of plasmid DNA using restriction enzymes, and agarose gel electrophoresis were carried out using standard methods (23). Plasmid DNA was introduced into bacterial cells by electrotransformation as described previously (11). Plasmid DNA was purified from *E. faecalis* as previously described (13, 35). Restriction enzymes were purchased from New England Biolabs and Roche Co. The PCR was performed with a Perkin-Elmer Cetus machine. Specific primers were purchased from Invitrogen. *rTaq* DNA polymerase and KOD plus DNA polymerase for PCR amplification were obtained from Takara Bio Co. (Tokyo, Japan) and Toyobo (Tokyo, Japan). PCR was carried out using *Taq* and the following parameters: 1 min at 95°C, 1 min at 56°C, and 2 min at 72°C for 30 cycles. PCR was carried out using KOD plus and the following parameters: 15 s at 94°C, 30 s at 60°C, and 1 min/kb at 68°C for 35 cycles. All plasmid constructs generated by PCR and in-frame deletion mutations in plasmids were confirmed by sequence analysis. To examine the plasmid constructs used in this study, sequence analysis was performed using the Dye primer and Dye terminator cycle sequencing kit (Applied Biosystems) and a 377 DNA sequencer and 310 Gene Analyzer (ABI Prism).

Conjugation experiments. Broth mating and solid surface mating were performed as previously described (6, 7, 16) with a donor/recipient ratio of 1:10. Broth matings (in THB) were carried out for 5 h, and solid surface matings (on THB agar plates) were carried out overnight (16 h). Transfer frequencies were calculated as the number of transconjugants per donor cell (at the end of mating).

Complementation study of pHTβ::Tn*917-lac* insertion mutants of Tra II region. Complementation studies of the Tn*917-lac* insertion mutants of the Tra II region were performed using the pAM401-based clones of the region (Table 1; see also Fig. S1 in the supplemental material). ORF56 and ORF57 in the Tra II region were cloned into the shuttle plasmid pAM401 utilizing PCR amplification (see Fig. 5 and also Fig. S3 in the supplemental material). The PCR primer sets used to clone the ORFs are shown in Table 2. Each of the pAM401 derivatives carrying the ORFs was introduced by electrotransformation into *E. faecalis* UV202, which is defective in homologous recombination (37, 39). Then, each pHTβ::Tn*917-lac* insertion mutant was introduced into each of the UV202 transformants carrying the pAM401 derivatives. Both broth mating and solid surface

TABLE 1. Bacterial strains and plasmids

Strain or plasmid	Relevant features	Reference or source
Strains		
E. faecalis		
FA2-2	*rif fus*	5
JH2SS	*spc str*	28
UV202	*rif fus*, recombination-deficient mutant of JH2-2	37, 39
OG1X	*str*	15
OG1RF	*rif fus*	6
OG1SS	*spc str*	10
E. faecium		
BM4105RF	*rif fus*	33
BM4105SS	*spc str*	33
E. coli		
DH5α	*endA1 recA1 gyrA96 thi-1 hsdR17 supE44 relA1* Δ(*argE-lacZYA*)*U169*	Bethesda Research Laboratories
TH688	CSH57b *thr*::Tn*5*	25
Plasmids		
pBluescript SKII(+)	*E. coli* cloning vector; Amp^r *lacZ*	Stratagene
pMW119	*E. coli* cloning vector; Amp^r *lacZ*	Nippon Gene Co.
pAM401	*E. coli-E. faecalis* shuttle vector; *cat tet*	38
pMGS100	pAM401-based shuttle vector; overexpression of promoterless gene by *bacA* promoter of bacteriocin 21	12
pAM2125	Tn*917-lac* insertion mutant of pAD1	36
pDL274	*E. coli-E. faecalis* shuttle; *aad(9)*	8
pTV32Ts	Transposon delivery vector, temperature sensitive; pE194Ts(Cm^r)::Tn*917-lac*(Em^r)	22
pHTβ	pMG1-like vancomycin resistance (Tn*1546*) conjugative plasmid	34
pHTβ::Tn*917-lac*/265, -/80, -/82, -/106	Tn*917-lac* insertion mutants of ORF56 (Tra II region) of pHTβ	32
pHTβ::Tn*917-lac*/136	Tn*917-lac* insertion mutant of ORF10 (Tra I region) of pHTβ	32
pHTβ::Tn*917-lac*/154	Tn*917-lac* insertion mutant of ORF13 (Tra I region) of pHTβ	32
pBS::ORF56del	pBS derivative carrying ORF56 with in-frame deletion	This study
pBS::ORF57del	pBS derivative carrying ORF57 with in-frame deletion	This study
pBS::ORF56/57del	pBS derivative carrying ORF56 and ORF57 with in-frame deletions	This study
pBS::ORF10del	pBS derivative carrying ORF10 with in-frame deletion	This study
pBS::ORF56del-Spc	pBS derivative carrying ORF56 with in-frame deletion and *aad(9)* gene of pDL274	This study
pBS::ORF57del-Spc	pBS derivative carrying ORF57 with in-frame deletion and *aad(9)* gene of pDL274	This study
pBS::ORF56/57del-Spc	pBS derivative carrying ORF56 and ORF57 with in-frame deletions and *aad(9)* gene of pDL274	This study
pBS::ORF10del-Spc	pBS derivative carrying ORF10 with in-frame deletion and *aad(9)* gene of pDL274	This study
pMG1000	pHTβ derivative mutant carrying an in-frame deletion of ORF56 (*traB*)	This study
pMG1001	pHTβ derivative mutant carrying an in-frame deletion of ORF57 (*traA*)	This study
pMG1002	pHTβ derivative mutant carrying an in-frame deletions of ORF56 (*traA*) and ORF57 (*traB*)	This study
pMG1003	pAM401 derivative plasmid carrying ORF56 (*traB*)	This study
pMG1005	pAM401 derivative plasmid carrying ORF56 (*traB*) and ORF57 (*traA*)	This study
pMG1007	pAM401 derivative plasmid carrying ORF56 (*traB*)	This study
pHT*lac*	pAM401 derivative plasmid carrying promoterless *lacZ* gene of pTV32Ts plasmid; Cm^r	This study
pMG1021	pHT*lac* derivative plasmid carrying ORF56 (*traB*) with P1, P2, and P3 promoter regions	This study
pMG1022	pHT*lac* derivative plasmid carrying ORF56 (*traB*) with P2 and P3 promoter regions	This study
pMG1023	pHT*lac* derivative plasmid carrying ORF56 (*traB*) with P3 promoter region	This study
pMG1024	pHT*lac* derivative plasmid carrying ORF56 (*traB*) without the deduced promoter region	This study

Continued on following page

TABLE 1—*Continued*

Strain or plasmid	Relevant features	Reference or source
pMG1025	pHT*lac* derivative plasmid carrying a part of ORF56 (*traB*) with P3 promoter region	This study
pMG1008	Tn*917-lac* insertion mutant of ORF10 (pHTβ::Tn*917-lac*/136) with in-frame deletion of *traB*	This study
pMG1009	Tn*917-lac* insertion mutant of ORF13 (pHTβ::Tn*917-lac*/154) with in-frame deletion of *traB*	This study
pMG1010	pHTβ derivative mutant carrying an in-frame deletion of ORF10	This study
pWM119/113	pMW119 derivative plasmid carrying HindIII fragments and containing ORF2 to ORF13 of pHTβ	32
pWM119/113K	pMW119/113-based derivative plasmid with deletion of a KpnI fragment	This study
pWM119/73	pMW119 derivative plasmid carrying HindIII fragments and containing ORF11 to ORF13 of pHTβ	32
pHT1010	pAM401-based chimera plasmid fused with pMW119/113 carrying ORF2 to ORF13 of pHTβ	This study
pHT1011	pAM401-based chimera plasmid fused with pMW119/113K carrying ORF7 to ORF13 of pHTβ	This study
pHT1011-38, -170, -120, -147, -112, -172, -16, -20, -23, -2, -84, -4	Tn*5* insertion mutants of pHT1011	This study
pMG1012	pHT1011-based derivative plasmid with deletion of a HindIII fragment	This study
pMG1013	pAM401 derivative plasmid carrying an MfeI fragment containing ORF9 to ORF13	This study
pMG1015	pHT1011-based derivative plasmid with deletion of a HindIII fragment	This study
pMG1016	pAM401-based chimera plasmid fused with pMW119/73 carrying ORF11 to ORF13 of pHTβ	This study
pMG1017 (pMGS100::ORF13)	pMGS100 derivative plasmid carrying ORF13 under the *bacA* promoter region of bacteriocin 21	This study
pMG1026	pHT*lac* derivative plasmid carrying P1, P2, and P3 promoter regions for ORF9	This study
pMG1027	pHT*lac* derivative plasmid carrying P3 promoter region for ORF9	This study
pMG1028	pHT*lac* derivative plasmid carrying upstream region of ORF9 without the deduced promoter region	This study
pMG1029	pHT*lac* derivative plasmid carrying internal region between ORF9 and ORF10	This study
pMG1030	pHT*lac* derivative plasmid carrying upstream region of ORF11	This study
pMG1	Pheromone-independent highly conjugative gentamicin resistance plasmid isolated from *E. faecium* clinical strain	17, 27
pMG1100	pMG1 derivative mutant carrying an in-frame deletion of 71ORF1 (equivalent to *traB* of pHTβ)	This study
pMG1101	pMG1 derivative mutant carrying an in-frame deletion of 71ORF2 (*traA*)	This study

mating were performed using the transconjugants carrying the two plasmids as donor strains and JH2SS as a recipient strain.

Cloning of the aggregation determinant of pHTβ. To clone the determinants for the aggregation region of the pHTβ plasmid, the pMW119-based clone sets of pHTβ, which had been constructed in the previous study, were utilized (see Fig. 2A; Table 1) (32). The partially HindIII-digested fragments of pHTβ had been cloned into the vector plasmid pMW119 for nucleotide sequence analysis. The plasmid clones carrying HindIII segments of the Tra I region of pHTβ were digested by BamHI and ligated to the EcoRI-digested *E. coli-E. faecalis* shuttle vector pAM401. Each of the pAM401-pMW119 chimeric derivatives carrying the Tra I region of pHTβ that were to be tested for the formation of cell aggregate was introduced into *E. faecalis* FA2-2 by electrotransformation. The clone pHT1010 was constructed as a chimeric plasmid between pAM401 and the clone pMW119/113 (see Fig. 2A; Table 1) (32). Plasmid pMW119/113K, a KpnI fragment deletion derivative of pMW119/113, was generated by digestion with KpnI followed by self-ligation of pMW119/113. pHT1011 was a chimeric plasmid formed between pMW119/113K and pAM401, with the two plasmids fused at the EcoRI site. The deletion derivatives pMG1012, pMG1015, and pMG1016 were constructed by partial deletion of the HindIII fragments of pHT1011. The clone pMG1013 was constructed by cloning the 6.0-kbp MfeI fragment that lies between 5.6 kbp and 11.6 kbp on the pHTβ map. The fragment was prepared from pHT1011 plasmid DNA by treatment with the MfeI enzyme and subcloning into the EcoRI site of pAM401. pMG1016 was constructed by plasmid fusion between pAM401 and pMW119/73 at the BamHI site. The coding region of ORF13 was cloned into the pAM401-based overexpression shuttle vector pMGS100 and was placed under a constitutively active *bacA* promoter for bacteriocin 41 derived from pPD1 plasmid (see Fig. 2A; Table 1) (12, 31). The 447-bp PCR product containing ORF13 was amplified by the primer set V11057F-V11513R and cloned into the EagI and NruI sites of pMGS100 to be overexpressed. The ORF13-expressed clone was designated pMG1017 (pMGS100::ORF13) (see Fig. 2A).

Generation of transposon (Tn*5*) insertion mutants. Tn*5* (Km^r) insertion into the cloned plasmid DNA was performed as described elsewhere (30, 31). The target plasmid pHT1011 (chimera plasmid of pAM401 with pWM119/113K containing the aggregation determinant region [see Fig. 2]) was introduced into *E. coli* K-12 TH688 (with Tn*5* in the *thr* locus) by electrotransformation (25). Ten transformants were spread onto selective plates containing kanamycin and chloramphenicol, and the plates were left at room temperature for 10 days. The bacteria that grew on the selective plates were pooled, and the plasmid DNA was then isolated and used to transform *E. coli* DH5α. The transformants were spread on plates containing kanamycin and chloramphenicol for the selection of Tn*5*-mediated kanamycin resistance and plasmid-mediated chloramphenicol re-

TABLE 2. Oligonucleotides used in this study

Oligonucleotide	Sequence (5′–3′)[a]	Plasmid(s) generated using this primer or used for RT-PCR analysis and Northern analysis
V46696F	GGCGGATCCAGAGTGAGAATATGTGGGAGC	pMG1003 (TraB clone), pMG1005 (TraB/TraA clone)
V47804R	GCCGGATCCGAGCGATAACGACTCTTTGCC	pMG1003, pMG1007, pMG1021, pMG1022, pMG1023, pMG1024 (TraB clones)
V48782R	GCCGGATCCATTTTCAGGCTACTTGTAGTC	pMG1005 (TraB/TraA clone)
V46548F	CCGGAATTCGGAGAATGAATGTGAAGCAGTGG	pBS::ORF56del (TraB internal deletion), pBS::ORF57del (TraA internal deletion), pBS::ORF56/57del (TraB-TraA internal deletion)
traBdelF1	TATCAGAGTACGTTAAGTCGGCGGTTTAAGGGG AGTAGGA	pBS::ORF56del (TraB internal deletion), pBS::ORF56/57del (TraB/TraA internal deletion)
traBdelR1	TCCTACTCCCCTTAAACCGCCGACTTAACGTACT CTGATA	pBS::ORF56del (TraB internal deletion)
traAdelF1	GCGGTTTAAGGGGAGTAGGAGTAGACAGGGCA CAGTTTTA	pBS::ORF57del (TraA internal deletion)
traAdelR1	TAAAACTGTGCCCTGTCTACTCCTACTCCCCTTA AACCGC	pBS::ORF57del (TraA), pBS::ORF56/57del (TraB/TraA internal deletion)
V48712R	GGCGAATTCGTTAGTCTTCTGTACGGCCCA	pBS::ORF56del (TraB internal deletion), pBS::ORF57del (TraA internal deletion), pBS::ORF56/57del (TraB/TraA internal deletion)
V6793F	GCCGGATCCTAATCACTTTATCAACGGCTC	pBS::ORF10del (ORF10 internal deletion)
ORF10delF	GGTTGGGCTAATAATGATGCCCATATGTCGCTT GATTTACCT	pBS::ORF10del (ORF10 internal deletion)
ORF10delR	AGGTAAATCAAGCGACATATGGGCATCATTATT AGCCCAACC	pBS::ORF10del (ORF10 internal deletion)
V10352R	GGCGGATCCAACCATCTGGTAGAGTAGACT	pBS::ORF10del (ORF10 internal deletion)
V46705F	TTTTAGCATGCTAATTTATTTAGTTTTATACTTAA TAGG	pMG1021 (TraB clone with P1, P2, and P3 promoters)
V46865F	TTTTAGCATGCTAGAATTATAATCACAAACTTAA TAGTAA	pMG1022 (TraB clone with P2 and P3 promoters)
V47025F	TTTTAGCATGCACGAAATAAATTTTAATTGAGG TTGAATT	pMG1023 (TraB clone with P3 promoter), pMG1025 (TraB clone with P3 promoter)
V47145F1	TTTTAGCATGCGGGTAGTTAAATTCGTAGATCA AAAGGC	pMG1024 (TraB clone without promoter)
V47582R	GCCGGATCCATCATAAAAAATTCCAAAAAG	pMG1025 (TraB clone with P3 promoter)
V47026F	GGCGGATCCACGAAATAAATTTTAATTGAGGTT GAATT	pMG1007 (TraB clone with P3 promoter)
V5783F	GCCGCATGCAGATAAAAGGCTGATTGTTCCGG	pMG1026 (P1, P2, and P3 promoter regions for ORF9)
V5932F	GCCGCATGCTATCAGGTTGATAGAAATTGTC	pMG1027 (P2 and P3 promoter regions for ORF9)
V5979F	GCCGCATGCTGATTTAGTAAAAAAATTAAA GGAG	pMG1028 (upstream region of ORF9 without the deduced promoter region)
V6189R	GGCGGATCCAAGCTGTACAAATAGACC	pMG1026, pMG1027, pMG1028 (promoter regions for ORF9)
V6298F	GCCGCATGCTTACTGTAAAGATAAGGGAATC	pMG1029 (internal region between ORF9 and ORF10)
V6841R	GGCGGATCCTTCAGCCGAAACAACTGATTGGC	pMG1029 (internal region between ORF9 and ORF10)
V10353F	GCCGCATGCAAAAATGAGATTGATTGGCTG	pMG1030 (upstream region of ORF11)
V10605R	GGCGGATCCGTGAATACCATTGAGTTTAATT	pMG1030 (upstream region of ORF11)
V11067F	TTTTTCGGCCGGAAGTGATGTAATGCTAAGAG	pMG1017 (ORF13 clone derivative of the overexpression shuttle vector pMGS100)
V11513R	ATTTTTCGCGATTTTTGAAGAAATTTTCTTTTCC	pMG1017 (ORF13 clone derivative of the overexpression shuttle vector pMGS100)
V47337F(traBF)	TTTGGTGGTATGGCAAGATGGTAC	RT-PCR for the internal region between *traB* and *traA*
V47959R(traAR)	AGCATTGCTCCATCCTACTCTAGC	RT-PCR for the internal region between *traB* and *traA*
V6311F(ORF9F)	GATAAGGGAATCATGATTCCAGCC	RT-PCR for "a" segment of ORF9-ORF10 region shown in Fig. 2C
V6800R(ORF10R)	TGATTAGGCTGAATAGAGCAACGC	RT-PCR for "a" segment of ORF9-ORF10 region shown in Fig. 2C
V10331F(ORF10F)	TCTACTCTACCAGATGGTTGGAGC	RT-PCR for "b" segment of ORF10-ORF11 region shown in Fig. 2C
V10610R(ORF11R)	ACCATATCCGTGAATACCATTGAG	RT-PCR for "b" segment of ORF10-ORF11 region shown in Fig. 2C
V10680F(ORF11F)	TCAAGTTGTGGCCTTTCTTGTGAG	RT-PCR for "c" segment of ORF11-ORF12 region shown in Fig. 2C
V10978R(ORF12R)	GTGGAATTAACCTAAGTTTGTAGGG	RT-PCR for "c" segment of ORF11-ORF12 region shown in Fig. 2C

Continued on following page

TABLE 2—*Continued*

Oligonucleotide	Sequence (5′–3′)[a]	Plasmid(s) generated using this primer or used for RT-PCR analysis and Northern analysis
V10889F(ORF12F)	GGAACAGCTAAAGTAGCTTTTCCTG	RT-PCR for "d" segment of ORF12-ORF13 region shown in Fig. 2C
V11104R(ORF13R2)	ATCATTTTGGGCATATCTCTTAGC	RT-PCR for "d" segment of ORF12-ORF13 region shown in Fig. 2C
V11393F(ORF13F)	TAAAGTGAAGGTTGAAAGTGGATC	RT-PCR for "e" segment of ORF13-ORF14 region shown in Fig. 2C
V11860R(ORF14R)	AATTCGCTCAATAATCCCTGTTCC	RT-PCR for "e" segment of ORF13-ORF14 region shown in Fig. 2C
V5999F	AAGGAGTGATAGCTGTTGGC	RNA probe specific to ORF9 used for Northern analysis shown in Fig. 2C
V6454R	CGCATAATACGACTCACTATAGGGAGAAATAAC AGTATGCTTGGTTGC	RNA probe specific to ORF9 used for Northern analysis shown in Fig. 2C
V11063F	GGATGGAAGTGATGTAATGC	RNA probe specific to ORF13 used for Northern analysis shown in Fig. 2C
V11503R	CGCATAATACGACTCACTATAGGGAGAATTTT CTTTTCCTCTACAACACG	RNA probe specific to ORF13 used for Northern analysis shown in Fig. 2C

[a] Underlines indicate the following restriction endonuclease recognition sequences for cloning or the T7 RNA polymerase promoter sequences: GGATCC, BamHI; GAATTC, EcoRI; GCATGC, SphI; CGGCCG, EagI; TCGCGA, NruI; TAATACGACTCACTATAGGGAGA, T7 RNA polymerase promoter sequences.

sistance, respectively. The transformants were purified and examined to determine the location of Tn*5* within the plasmid. The precise locations of Tn*5* insertion were determined by DNA sequence analysis using a synthetic primer that hybridized to the end of Tn*5*.

Construction of plasmid chimeras for use in complementation studies. The pAM401 derivative plasmids, pMG1003 (TraB clone), pMG1004 (TraA clone), pMG1005 (TraB/TraA clone), and pMG1007 (TraB clone), were constructed using PCR and the primers shown in Table 2. BamHI sites were incorporated into the 5′ termini of the primers to enable cloning into the BamHI sites of the shuttle vector pAM401. pMG1021 (TraB clone with P1, P2, and P3 promoter regions), pMG1022 (TraB clone with P2 and P3 promoter regions), pMG1023 (TraB clone with P3 promoter region), pMG1024 (TraB clone without promoter regions), and pMG1025 (N-terminal deletion in TraB clone with P3 promoter region) were constructed using PCR and the primers shown in Table 2. The SphI and BamHI sites were incorporated into the 5′ termini of the forward primer and the reverse primer, respectively, to enable cloning into the SphI and BamHI sites of the pAM401-based *lacZ* reporter assay vector pHT*lac* (described below).

Beta-galactosidase (LacZ) assay. LacZ activities were determined as previously described (29, 35), with the following minor modifications. One hundred microliters of an overnight culture of the appropriate strain was subcultured in 2.5 ml of fresh THB medium and grown for 4 h at 37°C. Cells were harvested from 0.7-ml aliquots and then suspended in 0.2 ml of 50 mM sodium phosphate buffer (pH 7.5) and permeabilized with 0.1 ml of toluene for 15 min at 37°C. Samples were incubated in 0.1 ml of 32 mM reduced glutathione, 0.25 ml of 10 mM *o*-nitrophenyl-β-D-galactopyranoside (ONGP), and 2.0 ml of 50 mM sodium phosphate (pH 7.5) for 30 min at 37°C. The reaction was stopped with 0.5 ml of 1 M Na_2CO_3, and cell debris was removed by centrifugation. Absorbency was determined at 420 nm on a DU640 spectrophotometer (Beckman), and the results were expressed in Miller units (MU) (20). *E. faecalis* FA2-2 or OG1X containing the pAM2125 plasmid was used as an internal control for this assay (36).

Construction of the ORF56 (*traB*) in-frame deletion mutation in pHTβ, pHTβ::Tn*917-lac*/136, and pHTβ::Tn*917-lac*/154. The overlapping PCR technique was used to construct the ORF56 (*traB*) deletion mutant of pHTβ and its derivatives as previously described (29, 32). The ORF56/ORF57 region containing a 498-bp deletion corresponding to 166 amino acid residues lying between the 20th and 185th residues of ORF56 was amplified by the overlapping PCR method using the specific primer sets (see Fig. 6; Table 2; see also Fig. S3 in the supplemental material). Two first-round PCRs were performed using the V46548F/traBdelR1 and traBdelF1/V48712R primer sets, and the following second-round PCR was performed using the V46548F/V48712Ra primer set. The amplified DNA fragment running from bp 46548 to 48712 on the map, which had an ORF56 (*traB*) internal deletion, was cloned into the EcoRI site of the pBluescript vector plasmid to form pBS::ORF56del (TraB/TraA clone with TraB internal deletion). A 1.1-kbp DNA fragment carrying a spectinomycin resistance gene [*aad(9)*] (8, 19, 27) was amplified by PCR and cloned into the SmaI site of pBS::ORF56del to give pBS::ORF56del-Spc. pBS::ORF56del-Spc was introduced into *E. faecalis* FA2-2/pHTβ by electrotransformation, and recombinants occurring via double homologous recombination were selected as previously described (29, 32). A representative recombinant carrying a 498-bp deletion of ORF56 (*traB*) was designated pMG1000. pHTβ::Tn*917-lac*/136 and pHTβ::Tn*917-lac*/154, the in-frame deletion mutants of ORF56 (*traB*), were obtained by the same strategy. The mutants were designated pMG1008 and pMG1009, respectively.

Construction of the ORF57 (*traA*) in-frame deletion mutation and the ORF56/57 (*traB/traA*) deletion mutation in pHTβ. The method described above was used to generate the ORF57 (*traA*) in-frame deletion mutant and ORF56/57 (*traA/traB*) double deletion mutant, except that the following primer sets were used (two first-round PCRs, V46548F/traAdelR1 and traAdelF1/V48712R; second-round PCR, V46548F/V48712R for *traA* deletion; two first-round PCRs, V46548F/traBdelR1 and traAdelF1/V48712R; second-round PCR, V46548F/V48712R for *traB/traA* deletion, respectively). The resulting plasmids were designated pMG1001 (*traA* in-frame deletion mutant of pHTβ) and pMG1002 (*traB/traA* in-frame deletion mutant of pHTβ), respectively (see Fig. 6). The intermediate recombinant plasmids (pBS::ORF57del and pBS::ORF57del-Spc or pBS::ORF56/57del and pBS::ORF56/57del-Spc, respectively) were also generated by this method (Tables 1 and 2).

Construction of the 71ORF2 (*traA*) in-frame deletion mutation and the 71ORF1 (equivalent to *traB* gene of pHTβ) in-frame deletion mutation in pMG1. The method described above and the recombinant plasmids (pBS::ORF57del-Spc and pBS::ORF56del-Spc) were used to generate the 71ORF2 (*traA*) in-frame deletion mutant and 71ORF1 (equivalent to *traB* gene of pHTβ) in-frame deletion mutant in pMG1 (Tables 1 and 2). The mutations were confirmed by PCR amplification and DNA sequences using the primer sets for 71ORF1 and 71ORF2, respectively. The mutants were designated pMG1101 (71ORF2 [*traA*] in-frame mutant of pMG1) and pMG1100 (71ORF2 [equivalent of *traB* of pHTβ] in-frame mutant of pMG1), respectively.

Construction of the ORF10 in-frame deletion mutation in pHTβ. The same strategy described above was used to generate the ORF10 in-frame deletion mutant, except that the following primer sets were used (two first-round PCRs, V6793F/ORF10delR and ORF10delF/V10352R; second-round PCR, V6793F/V10352R for ORF10 deletion). The resulting plasmid was designated pMG1010 (ORF10 in-frame deletion mutant of pHTβ) containing an 1,899-bp deletion corresponding to 633 amino acid residues lying between the 291st and 923rd residues of ORF10 (see Fig. 2D). The intermediate recombinant plasmids (pBS::ORF10del and pBS::ORF10del-Spc) were also generated by this method (Tables 1 and 2).

Construction of a pAM401-based *lacZ* reporter assay vector, pHT*lac* (Cm^r), for enterococci. To analyze the promoter regions of ORF56 (*traB*) and ORF9, a new vector plasmid was constructed from the shuttle vector pAM401 (see Fig. 3) (38). pTV32Ts plasmid DNA (15.6 kbp) was digested with AflII and then blunted by treatment with Klenow enzyme (22). The blunted DNA was digested with BamHI, and a 3.2-kbp BamHI/AflII (blunted) DNA fragment containing the promoterless *lacZ* gene from the pTV32Ts plasmid was isolated and purified

from an agarose gel after electrophoresis. pAM401 plasmid DNA (10.4 kbp) was partially digested with HindIII and then blunted by treatment with Klenow enzyme. The blunted DNA was digested with BamHI, and the 10.1-kbp BamHI/HindIII (blunted) fragment lacking an 0.3-kbp BamHI/HindIII fragment was isolated and purified from an agarose gel after electrophoresis. The 3.2-kbp BamHI/AflII (blunted) fragment of pTV32Ts and the 10.1-kbp BamHI/HindIII (blunted) fragment were ligated, and the circular DNA was then introduced into DH5α by electrotransformation. The desired pAM401 derivative plasmid carrying a promoterless *lacZ* gene was selected and designated pHT*lac* (13.3 kbp). The amplified PCR products carrying the ORF56 (*traB*) region were cloned into the SphI and BamHI sites of pHT*lac*, and the transcription levels were determined by measuring LacZ activity. The amplified PCR products containing the upstream region of ORF9 were also cloned into the SphI and BamHI sites of pHT*lac*, and the transcription level was examined by determining LacZ activity.

RNA preparation from the *E. faecalis* strain and RT-PCR analysis. Cells were grown at 37°C overnight in THB. Cells were treated with a solution of lysozyme (50 mg/ml) and lysostaphin (Wako Chemicals, Osaka Japan) at 37°C for 30 min, and total RNA was extracted using the Fast RNA Red kit (Bio 101) and FastPrep (Savant). Reverse transcription-PCR (RT-PCR) analysis was performed following the protocol for the Access RT-PCR system (Promega Co., Madison, WI) with primer pairs designed to amplify two ORFs (ORF9 to ORF14) in the pHTβ Tra I region. Prior to use in RT-PCR, the extracted RNA was treated with RNase-free DNase I (Promega). An 0.5-μg quantity of RNA and 50 pmol of each primer were used in each RT-PCR. Each fragment was amplified as follows: 45°C for 45 min for reverse transcription, followed by inactivation of avian myeloblastosis virus reverse transcriptase and denaturation of the template at 94°C for 2 min. The program was set at 94°C for 30 s, 60°C for 90 s, and 68°C for 2 min for 40 cycles and terminated by a final elongation step of 7 min. Control reactions were performed with RNA from the plasmid-free isogenic strain without template RNA and also with template RNA but omitting the reverse transcription step. RT-PCR products were analyzed on 1.2% agarose gels.

Northern hybridization analysis and in vitro transcription. Northern hybridization analysis was performed following the protocol for the digoxigenin (DIG) nonradioactive system (Boehringer Mannheim). The contamination by DNA of the extracted total RNA samples was checked by the RT-PCR method described above. The repeated treatment with RNase-free DNase (Boehringer Mannheim) was performed to remove the DNA from the sample when required. Then, the extract was diluted with 4 volumes of RNA loading buffer (50% formamide, 2% formaldehyde, 0.01% bromophenol blue, 10% glycerol, 20 mM morpholinepropanesulfonic acid [MOPS]) and separated on an 0.8% agarose gel containing 2% formaldehyde and MOPS buffer at 40 V for 3.5 h. After the extract was transferred onto a nylon membrane (Boehringer Mannheim), the membrane was incubated in DIG Easy Hyb solution (Boehringer Mannheim) at 68°C for several hours and hybridized with DIG-labeled RNA probe overnight. The membrane was washed twice in 2× SSC (1× SSC is 0.15 M NaCl plus 0.015 M sodium citrate)-0.1% sodium dodecyl sulfate at room temperature for 5 min and then twice in 0.1× SSC-0.1% sodium dodecyl sulfate at 65°C for 15 min. The chemiluminescent substrate CDP-Star (Boehringer Mannheim) was used for visualization of the RNA bands. The chemiluminescence was detected using Lumi-Film (Boehringer Mannheim). The DIG-labeled RNA probes used in this study were generated by in vitro transcription. ORF9 and ORF13 were amplified by PCR using the specific primer sets shown in Table 2. The T7 RNA polymerase sequence 5′-TAATACGACTCACTATAGGGAGA-3′ was incorporated in the reverse primers to generate cRNA in vitro. The amplified ORF9 and ORF13 products were purified and used as the templates for the second-round PCR amplification using the same primer sets. The PCR products were used for the generation of RNA probes by a DIG-RNA labeling kit following the manufacturer's recommendations (Boehringer Mannheim).

RESULTS

Macroscopic self-aggregation of *E. faecalis* strains harboring pHTβ in broth culture. *E. faecalis* strains FA2-2 and OG1X harboring the pHTβ plasmid showed the macroscopic self-aggregation phenotype in broth culture (Fig. 1). Aggregation was weak, and cells were dispersed by intensive vortex mixing. Previously, Tn*917-lac* insertion mutants of pHTβ had been generated in an *E. faecalis* OG1X background (32). The transfer frequency of the 124 representative derivatives has been examined in broth mating between the *E. faecalis* strains

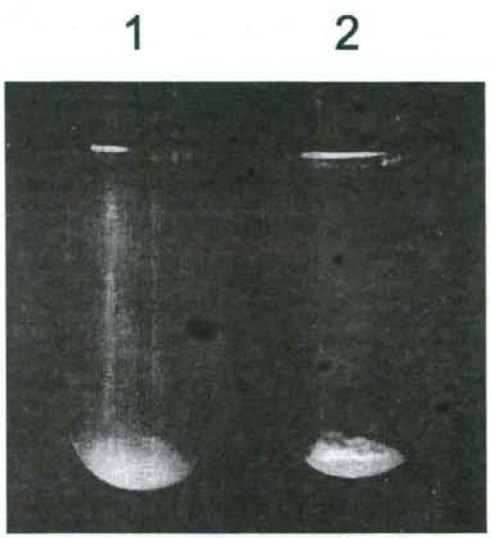

FIG. 1. Cell aggregation of *E. faecalis* strains carrying the pHTβ plasmid in liquid culture. The strains were incubated in THB medium overnight without shaking. 1, FA2-2 (no plasmid); 2, FA2-2(pHTβ).

FA2-2 and JH2SS and strains OG1RF and OG1SS (32). Tn*917-lac* insertion mutants that show a reduction in or loss of transfer frequency in broth mating were mapped to three transfer-related regions within the pHTβ plasmid (Tra I, II, and III) (see Fig. S1 in the supplemental material).

Representative pHTβ plasmid insertion mutants were transferred to FA2-2 strains from the original OG1X host strain by solid surface mating (filter mating), and each was examined for aggregation. Insertion mutants within Tra II, Tra III, and most of the upstream region of Tra I (that is, upstream of ORF17) transferred to the recipient strains. Insertion mutants within the downstream region of Tra I did not transfer at a frequency of more than 10^{-8} per donor cell, which indicated a complete lack of transferability. The FA2-2 or OG1X strain carrying insertion mutants in Tra II or most of the upstream region of Tra I showed weak aggregation or no aggregation compared to that of the wild-type strain. The strains carrying insertion mutants in the Tra III region showed self-aggregation. The results indicated that the Tra I and Tra II regions were involved in both plasmid transfer and cell aggregation. The results implied that the self-aggregation observed in the FA2-2 strains carrying pHTβ could be related to the formation of mating aggregates in plasmid transfer.

Cloning of aggregation determinants of pHTβ. To identify the genes required for the formation of cell aggregates related to plasmid transfer, the pHTβ plasmid clone sets that had been generated in our previous study were tested for their ability to produce aggregation in *E. faecalis* FA2-2 (32). The pHT1010 clone conferred the aggregation phenotype on the host strain (Fig. 2). Several derivatives of pHT1010 were constructed, and their aggregation-inducing abilities were examined (Fig. 2A). The derivative pMG1013 carrying the 6.0-kbp MfeI fragment that lies between 5.6 kbp

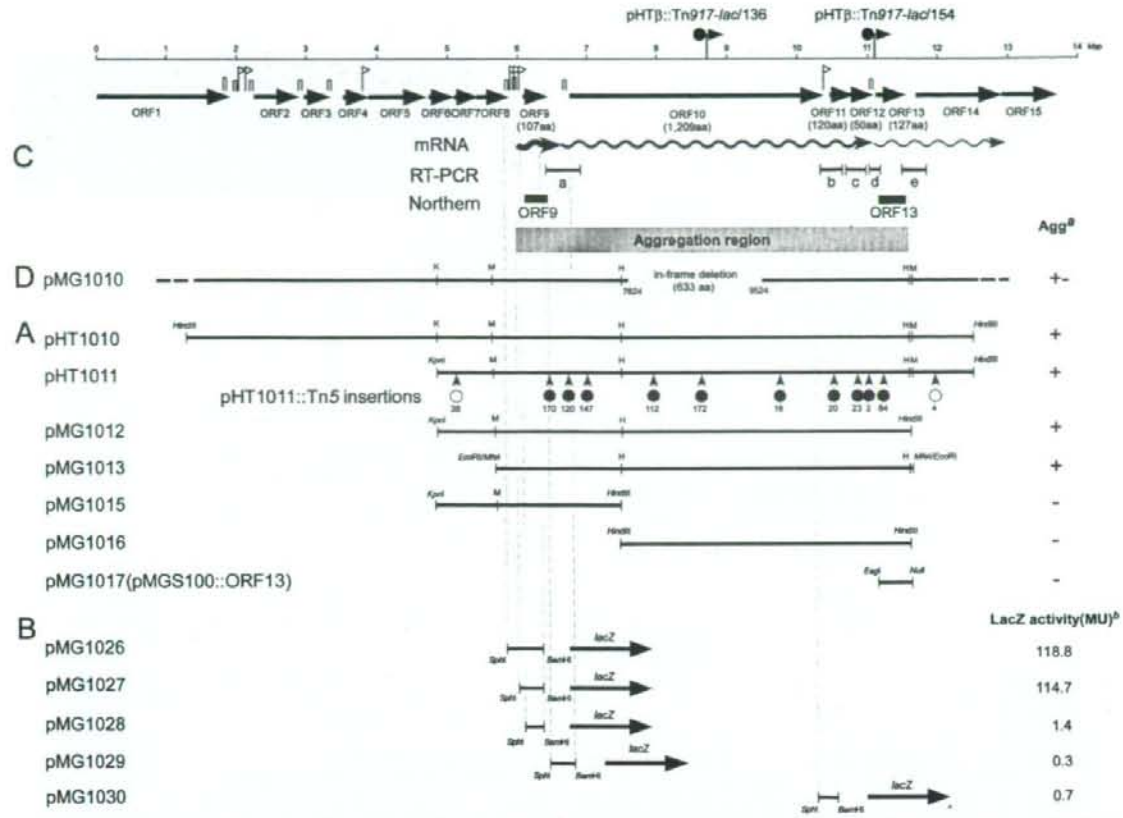

FIG. 2. Physical map of the aggregation-related region of pHTβ. The horizontal arrows indicate the deduced ORFs encoded on pHTβ. The flags with a white triangle indicate the potential promoter regions. The hairpins indicate the inverted repeat sequences. The two flags with a black triangle indicate the Tn*917-lac* insertion mutants of pHTβ and the direction of the inserts (*lacZ* gene). Each horizontal bar indicates the DNA segment of pHTβ carried by the plasmid clone. Small vertical bars on the horizontal bars indicate the restriction endonuclease recognition sites: H, HindIII; K, KpnI; M, MfeI. (A) The vertical arrows with circles indicate the Tn*5* insertion mutants of pHT1011. The color of the circle indicates the degree of aggregation phenotype of the mutants: white circle, same as that of the wild-type plasmid; black circle, no aggregation. *a*, plus sign indicates aggregation phenotype and minus sign shows nonaggregation phenotype. (B) Analysis of the promoter activity of the upstream region of ORF9 using a newly constructed *lacZ* reporter plasmid, pHT*lac* (Fig. 3). The three potential promoter regions, designated P1, P2, and P3, shown in Fig. S2 in the supplemental material were examined by the *lacZ* expression assay. *b*, activities were measured in FA2-2 strains in triplicate, and representative results are shown. Two internal regions, between ORF9 and ORF10 (pMG1029) and between ORF10 and ORF11 (pMG1030), were also examined for promoter activity. (C) The horizontal wavy line indicates the deduced transcriptional organization in the aggregation region of pHTβ. Each horizontal bar with the letters "a" to "e" under the transcript indicates the internal segment between each ORF amplified by RT-PCR analysis using the specific primer sets listed in Table 2. The results of RT-PCR analysis are shown in Fig. 4. The thick horizontal bars designated ORF9 and ORF13 indicate the RNA probes used for Northern hybridization analysis shown in Fig. 6. (D) FA2-2 strain carrying pMG1010 (ORF10 in-frame deletion mutant of pHTβ) showing the weak (reduced)-aggregation phenotype (+−).

and 11.6 kb on the map expressed the aggregation characteristic and contained five ORFs running from ORF9 to ORF13. The deletion mutant pMG1015, which contained only the complete ORF9, did not confer the aggregation phenotype, suggesting that ORF10 to ORF13 were necessary for aggregation. The deletion mutant pMG1016 contained the region ORF11 to ORF13 and did not confer the aggregation phenotype, suggesting that ORF9 or ORF10 (or both ORFs) might be necessary for aggregation. DNA sequence analysis showed that there were four good potential promoter regions in the pMG1013 fragment. Three potential promoters were located upstream of ORF9, and one was located in the upstream region of ORF12.

Analysis of Tn*5* insertion mutants in the aggregation region. Tn*5* insertion mutants of pHT1011, which contains the 7.7-kbp region from 4.8 kbp to 12.5 kbp on the pHTβ plasmid map, were generated for the detailed analysis of the aggregation determinants (Fig. 2A). Twelve Tn*5* insertion mutants were selected and examined for aggregation. Two of the mutants, −38 and −4, expressed the same level of aggregation as did the wild-type plasmid. The remaining 10 mutants showed no aggregation phenotype compared to the

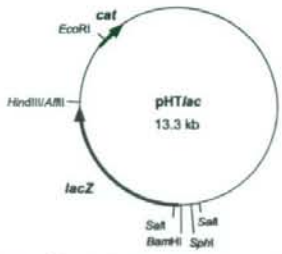

FIG. 3. Structure of the pAM401-based cloning vector plasmid carrying the promoterless *lacZ* gene of pTV32Ts (22) and designated pHT*lac* in this study. The construction of pHT*lac* is described in Materials and Methods. The 10.1-kbp BamHI/HindIII (blunted) segment containing *cat* was derived from pAM401, and the 3.2-kbp BamHI/AflII (blunted) segment containing *lacZ* was derived from pTV32Ts (22, 38).

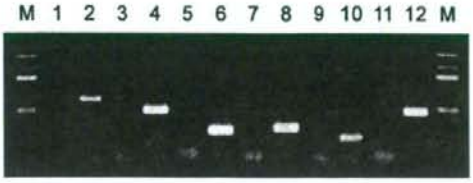

RT[a]	-	+	-	+	-	+	-	+	-	+	-	+
Region (in Fig. 2C[b])	*traB/traA*		ORF9/10 a		ORF10/11 b		ORF11/12 c		ORF12/13 d		ORF13/14 e	
Primer set	traBF traAR		ORF9F ORF10R		ORF10F ORF11R		ORF11F ORF12R		ORF12F ORF13R2		ORF13F ORF14R	
Size (bp)	623		490		280		299		216		468	

FIG. 4. RT-PCR analyses of the transcripts in the aggregation region and Tra II region of pHTβ in *E. faecalis* FA2-2 background. Lanes M, 100-bp ladder marker (New England Biolabs); lanes 1 and 2, *traB-traA* internal region (623 bp) amplified by primer set V47337F(traBF)/V47959R(traAR) without reverse transcriptase (lane 1) and with reverse transcriptase (lane 2); lanes 3 and 4, ORF9-ORF10 internal region (490 bp) amplified by primer set V6311F(ORF9F)/V6800R(ORF10R) without reverse transcriptase (lane 3) and with reverse transcriptase (lane 4) shown in Fig. 2C, "a"; lanes 5 and 6, ORF10-ORF11 internal region (280 bp) amplified by primer set V10331F(ORF10F)/V10610R(ORF11R) without reverse transcriptase (lane 5) and with reverse transcriptase (lane 6) shown in Fig. 2C, "b"; lanes 7 and 8, ORF11-ORF12 internal region (299 bp) amplified by primer set V10680F(ORF11F)/V10978R(ORF12R) without reverse transcriptase (lane 7) and with reverse transcriptase (lane 8) shown in Fig. 2C, "c"; lanes 9 and 10, ORF12-ORF13 internal region (216 bp) amplified by primer set V10889F(ORF12F)/V11104R(ORF13R2) without reverse transcriptase (lane 9) and with reverse transcriptase (lane 10) shown in Fig. 2C, "d"; lanes 11 and 12, ORF13-ORF14 internal region (468 bp) amplified by primer set V11393F(ORF13F)/V11860R(ORF14R) without reverse transcriptase (lane 11) and with reverse transcriptase (lane 12) shown in Fig. 2C, "e." *a*, RT, reverse transcriptase used for RT-PCR. *b*, each letter corresponds to the identical region shown in Fig. 2C.

wild-type plasmid clone in an *E. faecalis* background strain. The inserts in these 10 aggregation-deficit mutants were mapped to four ORFs lying between ORF10 and ORF13 or within the noncoding region between ORF9 and ORF10. Together with the results of the deletion mutant analysis, these results suggested that the five ORFs running from ORF9 to ORF13, including the predicted promoter region upstream of ORF9, were essential for cell aggregation in an FA2-2 background, although we could not exclude any potential polar effects on adjacent genes produced by the transposon insertions. The results of insertion mutagenesis of pHT1011 were consistent with those of the cloning experiments with the aggregation determinants.

Analysis of the transcription of the aggregation region. There were four potential promoter regions in the 6-kb aggregation region (Fig. 2). Three were located in the region upstream of ORF9, and these were designated P1, P2, and P3 (see Fig. S2 in the supplemental material), and one lay between ORF10 and ORF11. To examine promoter activity, a new shuttle vector plasmid called pHT*lac* containing the promoterless *lacZ* was constructed for the transcript reporter assay (Fig. 3). The activities of the three potential ORF9 promoters were genetically examined using the pHT*lac* plasmid (Fig. 2B). Each of the promoter regions was cloned into the pHT*lac* plasmid and was examined for promoter activity using *lacZ* expression. Both pMG1026 and pMG1027, which contained the P3 promoter region that lies closest to ORF9, showed strong promoter activity in the *lacZ* expression assay, but pMG1028, which did not carry P3, showed no activity (Fig. 2B). The results indicated that the P3 promoter region was constitutively active in the plasmid clone. Two other regions, the noncoding region between ORF9 and ORF10 and the upstream region of ORF11, were also examined for promoter activities using the pHT*lac* plasmid. The constructs were designated pMG1029 (carrying the noncoding region between ORF9 and ORF10) and pMG1030 (carrying the upstream region of ORF11 containing a potential promoter), respectively (Fig. 2B). Those LacZ activities were 0.3 and 0.7 MU, respectively, and neither construct showed significant promoter activities. The genetic analyses of the aggregation region implied that the five ORFs running from ORF9 to ORF13 formed an operon structure and had significant promoter activity in front of ORF9.

To examine transcription in this region, RT-PCR was performed with pHTβ as described in Materials and Methods using the five specific primer sets that amplify each internal region between the ORFs (Fig. 2C and 4). All primer sets gave the expected-size products, and the products were confirmed by DNA sequence analysis. The results showed that transcription started from P3 upstream of ORF9 and was read through all five ORFs forming the operon structure.

Cloning of ORF13 into the overexpression shuttle vector pMGS100. The genetic analysis showed that the aggregation region of pHTβ extended from ORF9 to ORF13 and that these five ORFs formed an operon structure. We could not exclude the possibility of polar effects by transposon insertions in the mutants, and there was a possibility that a single ORF13 gene would be the sole determinant of aggregation. To examine the possibility, the coding region of ORF13 with the deduced Shine-Dalgarno sequence was cloned into the overexpression shuttle vector pMGS100 as described in Materials and Methods (12). pMGS100 has a constitutively active promoter region for the *bacA* gene of bacteriocin 41 derived from pPD1, and promoterless genes could be cloned under the promoter region and overexpressed in *E. faecalis*

TABLE 3. Complementation study of pHTβ::Tn*917-lac* mutants in the Tra II region

Plasmid (insertion region/ORF)	Phenotype with complementary plasmid (aggregation/transfer frequency of broth mating/transfer frequency of solid surface mating)[a]			
	pAM401 (vector)	pMG1003 (ORF56 [*traB*])	pMG1005 (ORF56 [*traB*], ORF57 [*traA*])	pMG1007 (ORF56 [*traB*])[b]
pHTβ (wild type)	$Agg^+/9.3 \times 10^{-6}/7.0 \times 10^{-3}$	NT[c]	NT[c]	NT[c]
pHTβ::Tn*917-lac*/265 (Tra II/ORF56)	$Agg^-/<10^{-7}/3.3 \times 10^{-6}$	$Agg^+/4.4 \times 10^{-5}/3.1 \times 10^{-2}$	$Agg^+/2.8 \times 10^{-5}/2.0 \times 10^{-2}$	$Agg^+/1.8 \times 10^{-5}/7.0 \times 10^{-3}$
pHTβ::Tn*917-lac*/80 (Tra II/ORF56)	$Agg^-/<10^{-7}/1.8 \times 10^{-6}$	$Agg^+/1.8 \times 10^{-5}/1.4 \times 10^{-2}$	$Agg^+/1.2 \times 10^{-5}/1.2 \times 10^{-2}$	$Agg^+/1.2 \times 10^{-5}/1.4 \times 10^{-2}$
pHTβ::Tn*917-lac*/82 (Tra II/ORF56)	$Agg^-/<10^{-7}/8.0 \times 10^{-7}$	$Agg^+/1.1 \times 10^{-5}/1.1 \times 10^{-2}$	$Agg^+/1.9 \times 10^{-5}/1.9 \times 10^{-2}$	$Agg^+/8.3 \times 10^{-6}/7.9 \times 10^{-3}$
pHTβ::Tn*917-lac*/106 (Tra II/ORF56)	$Agg^-/<10^{-7}/6.4 \times 10^{-7}$	$Agg^+/1.5 \times 10^{-5}/8.6 \times 10^{-3}$	$Agg^+/9.1 \times 10^{-6}/7.6 \times 10^{-3}$	$Agg^+/1.1 \times 10^{-5}/5.0 \times 10^{-3}$

[a] The transfer frequency was calculated as the number of transconjugants per donor cell. The mating times were 5 h for broth mating and 16 h for solid surface mating. The matings were performed using UV202 strains carrying the two plasmids as donor strains and JH2SS as the recipient strain. These results are representative of at least three independent experiments.

[b] The smallest *traB* clone with a predicted P3 promoter region (Fig. 5; see also Fig. S3 in the supplemental material).

[c] NT, not tested.

strains (13, 31). The ORF13 clone of pMGS100 was generated and designated pMG1017. The FA2-2 strain containing pMG1017 showed no aggregation phenotype (Fig. 2A). The result indicated that ORF13 alone was not enough for the formation of self-aggregates, although the expression of ORF13 protein was not examined by biochemical analysis in this study.

Analysis of in-frame deletion mutants of ORF9 to ORF13 of pHTβ. To confirm whether each of five ORFs from ORF9 to ORF13 was necessary for the aggregation phenotype, we have tried to generate an in-frame deletion mutant of each of the ORFs in pHTβ. The ORF10 (1,209 amino acids) in-frame deletion mutant of pHTβ designated pMG1010 was successfully obtained in this study as described in Materials and Methods (Fig. 2D). The in-frame deletion mutant pMG1010 had an internal deletion of 633 amino acid residues lying between the 291st and 923rd residues of ORF10. pMG1010 conferred quite weak aggregation on the host FA2-2 strain, which was recognized only by careful observation (Fig. 2D). pMG1010 and pHTβ transferred at the frequencies of 4.3×10^{-7} and 5.4×10^{-6} per donor cell in broth mating, respectively. pMG1010 and pHTβ transferred at the frequencies of 1.5×10^{-3} and 2.1×10^{-3} per donor cell in solid surface mating, respectively. These results indicated that the ORF10 in-frame deletion mutation resulted in a decrease of the transfer frequency in broth mating (decreased to about 1/10 of that of the parent plasmid) but did not alter the transfer frequency in solid surface mating. This result suggested that the ORF10 product was associated with the formation of aggregates and that the macroscopic self-aggregation of pHTβ would be associated with mating aggregates for plasmid transfer.

Complementation study of Tn*917-lac* insertion mutants in the Tra II region of pHTβ. The transfer functions of the Tra II region were examined by complementation of the Tra II region with insertion mutants lying within this region (Fig. 5 and Table 3). All of the insertion mutants in the Tra II region were mapped either upstream of or within the internal region of ORF56 but not within ORF57 (*traA*), which corresponded to the *traA* gene of pMG1 (Fig. 5 and see Fig. S3 in the supplemental material) (26, 34). It is thought that *traA* of pMG1 might be involved in the formation or stabilization of the mating aggregate (26). The insertion mutants within the Tra II region of pHTβ plasmid lost both the ability to transfer plasmid and the ability to form cell aggregates (Table 3). The Tra II region contained three good potential promoter sequences upstream of ORF56 and a predicted Rho-independent terminator sequence just downstream of ORF57 (*traA*). ORF56 and ORF57 (*traA*) appear to form an operon structure and were transcribed as one transcript. Fragments containing ORF56, ORF56/57 with the three potential promoter sequences (P1, P2, and P3), or just ORF56 with the potential promoter P3 were cloned into pAM401 (38), and the cloned plasmids were named pMG1003, pMG1005, and pMG1007, respectively. pMG1003 and pMG1005 complemented each of the four representative insertion mutants pHTβ::Tn*917-lac*/265, pHTβ::Tn*917-lac*/80, pHTβ::Tn*917-lac*/82, and pHTβ::Tn*917-lac*/106 in ORF56 in *trans* (Fig. 5) (Table 3). pMG1007, which contained the predicted promoter P3 and ORF56, also complemented these four mutants (Table 3). These clones complemented both plasmid transfer and cell aggregation mutations. The results implied that ORF56 of the Tra II region was the transfer-related gene of the pHTβ plasmid.

Analysis of ORF56 of the Tra II region of the pHTβ plasmid. The results of the Tra II region complementation study implied that ORF56 might be a transfer-related gene encoding a deduced 187-amino-acid protein. To confirm this, in-frame deletion mutants of ORF56 and ORF57 were constructed in pHTβ and transferability and aggregation were analyzed as described in Materials and Methods (Fig. 5) (Table 4). An in-frame deletion mutant of ORF56, designated pMG1000, showed a transfer deficiency and no aggregation. An in-frame deletion mutant of ORF57, designated pMG1001, transferred at the same frequency as did the wild-type plasmid and conferred the ability to aggregate on the host cell. A deletion mutant of both ORF56 and ORF57, which was designated pMG1002, showed a phenotype identical to that of pMG1000. The ORF56 (pMG1003) and ORF56/ORF57 (pMG1005) clones could complement not only pMG1000 but also pMG1002 (data not shown). These results indicated that ORF56 was necessary for both plasmid transfer and cell aggregation, although the function of ORF57 (*traA*) in transfer has not yet been elucidated in pHTβ. ORF56 was designated

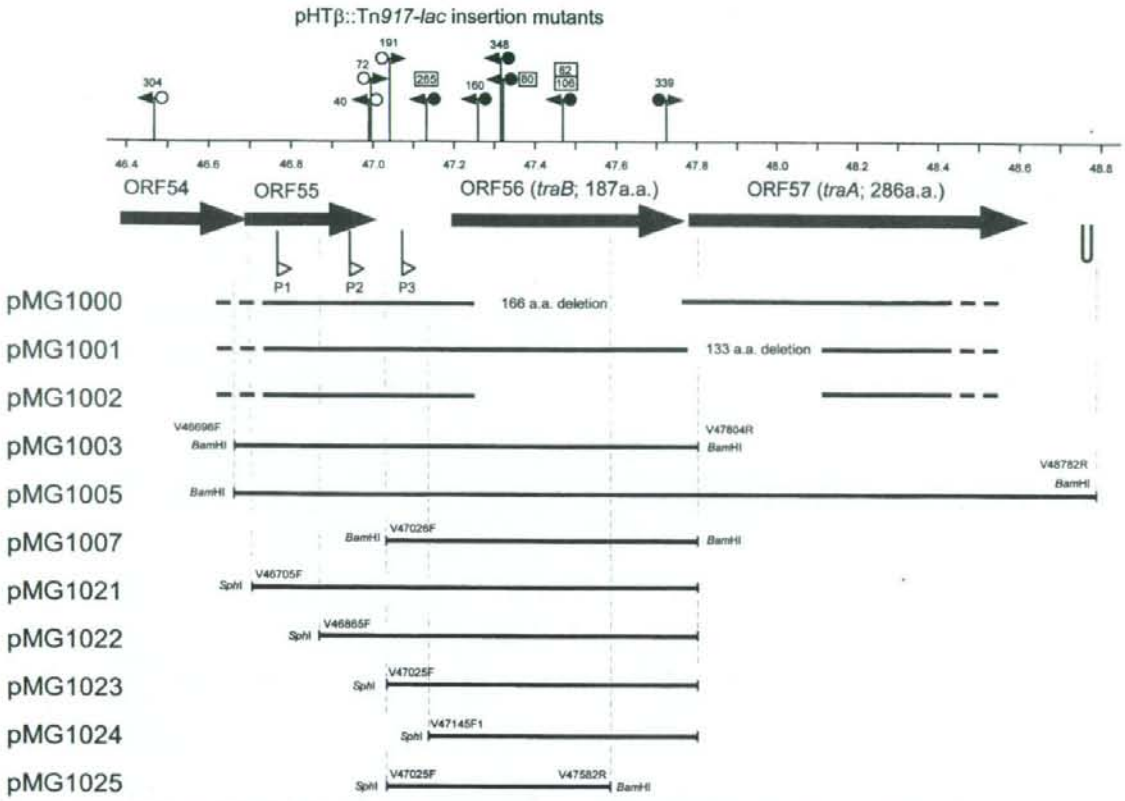

FIG. 5. Physical map of the Tra II region of pHTβ. The large horizontal arrows under the map show the ORFs and the direction of the transcript. Three flags (indicated as P1, P2, and P3) and a hairpin under the ORFs indicate the good potential promoter sequences and inverted repeat sequence, respectively. The small horizontal arrows with a circle and a number(s) on the map indicate the locations of Tn*917-lac* insertions and the direction of the *lacZ* gene. The colors of the circles indicate the transfer frequencies of the derivative plasmids: black, transfer-deficient mutants; white, transfer at the same frequency as that of the wild-type plasmid; light gray, transfer frequency of about one-third of that of the wild type; dark gray, transfer frequency lower than 10% of that of the wild type. Four marked insertion mutants, pHTβ::Tn*917-lac*/265, pHTβ::Tn*917-lac*/80, pHTβ::Tn*917-lac*/82, and pHTβ::Tn*917-lac*/106, were used in the complementation study for ORF56 (*traB*). The horizontal lines indicate the pHTβ segments of the clones or the structure of the in-frame deletion derivatives of the Tra II region. The small vertical lines at the ends of the horizontal lines indicate the endonuclease recognition sites. The names at the end of each horizontal line indicate the names of primers for the constructions.

traB. The deduced TraB protein of 187 residues showed 100% homology with 71ORF1 of pMG1 but no significant homology with any other reported gene products.

There were three potential promoter regions designated P1, P2, and P3 upstream of *traB* (Fig. 5 and see Fig. S3 in the supplemental material). As described above, the Tra II complementation study and the study of insertion mutants in the Tra II region implied that the predicted promoter P3 was sufficient for the expression of ORF56. The activities of the three potential promoters for the *traB* gene were genetically examined using the pHT*lac* plasmid (Fig. 5) (Table 4). The promoter regions from P1 to P3 with *traB* were cloned into the pHT*lac* plasmid, and the resulting plasmids were named pMG1021, pMG1022, and pMG1023; they contained the predicted promoter(s) P1/P2/P3, P2/P3, and P3, respectively. pMG1024 contained no promoter, and pMG1025 contained the P3 promoter and part of *traB*. Each of the cloned *traB* regions was examined for the ability to complement the in-frame pHTβ *traB* mutant pMG1000 and the promoter activity through *lacZ* expression. The three plasmids pMG1021, pMG1022, and pMG1023 containing the P3 promoter region closest to *traB* and the intact *traB* complemented transferability and aggregation of the *traB* mutant pMG1000 and showed *lacZ* expression in the promoter activity (Table 4). On the other hand, pMG1024 and pMG1025 did not complement transferability or aggregation. The results implied that the P3 promoter region was sufficient for *traB* transcription and that P3 was a constitutive promoter, although it is possible that the multicopy plasmid pAM401 had an effect on activity.

To examine the Tra II region transcript, RT-PCR was performed using the specific primers listed in Table 2 to amplify the internal region between *traB* and *traA*. The results con-

TABLE 4. In-frame deletion mutants of ORF56 (*traA*) and ORF57 (*traB*) and complementation study

Plasmid(s)[a]	Aggregation phenotype	Transfer frequency[b]		LacZ activity (MU)[c]
		Broth mating	Solid surface mating	
pHTβ (wild type)	+	5.4×10^{-6}	2.1×10^{-3}	NT[e]
pMG1000 (pHTβ; Δ*traB*)	−	$<1.1 \times 10^{-7}$	6.9×10^{-6}	NT
pMG1001 (pHTβ; Δ*traA*)	+	6.5×10^{-6}	6.0×10^{-3}	NT
pMG1002 (pHTβ; Δ*traA* Δ*traB*)	−	$<1.8 \times 10^{-7}$	1.2×10^{-5}	NT
pMG1007 (*traB* P3)[d]	−	NT	NT	NT
pMG1021 (*traB* P1, P2, P3)[d]	−	NT	NT	26.7
pMG1022 (*traB* P2, P3)[d]	−	NT	NT	32.7
pMG1023 (*traB* P3)[d]	−	NT	NT	39.4
pMG1024 (*traB*)	−	NT	NT	0.4
pMG1025 (part of *traB*; P3)[d]	−	NT	NT	45.2[f]
pMG1000 (pHTβ; Δ*traB*) + pMG1007 (*traB* P3)[d]	+	5.1×10^{-6}	2.3×10^{-2}	NT
pMG1002 (pHTβ; Δ*traA* Δ*traB*) + pMG1007 (*traB* P3)[d]	+	1.9×10^{-5}	4.5×10^{-2}	NT
pMG1000 (pHTβ; Δ*traB*) + pMG1021 (*traB* P1, P2, P3)[d]	+	1.0×10^{-5}	4.6×10^{-2}	23.9
pMG1000 (pHTβ; Δ*traB*) + pMG1022 (*traB* P2, P3)[d]	+	4.9×10^{-6}	8.6×10^{-2}	29.5
pMG1000 (pHTβ; Δ*traB*) + pMG1023 (*traB* P3)[d]	+	1.1×10^{-6}	4.7×10^{-3}	31.4
pMG1000 (pHTβ; Δ*traB*) + pMG1024 (*traB*)	−	$<1.9 \times 10^{-7}$	5.9×10^{-6}	0.2
pMG1000 (pHTβ; Δ*traB*) + pMG1025 (part of *traB*; P3)[d]	−	$<1.4 \times 10^{-7}$	9.0×10^{-6}	68.4[f]
pMG1	−	6.4×10^{-6}	6.0×10^{-3}	NT
pMG1100 (pMG1; Δ*traB*)	−	4.6×10^{-7}	3.3×10^{-4}	NT
pMG1101 (pMG1; Δ*traA*)	−	7.2×10^{-6}	4.9×10^{-3}	NT

[a] pMG1007, clone into vector pAM401; from pMG1021 to pMG1025, clone into pHT*lac* (Table 1 and Fig. 5; see also Fig. S3 in the supplemental material).
[b] The transfer frequency was calculated as the number of transconjugants per donor cell. The mating times were 5 h for broth mating and 16 h for solid surface mating. The matings were performed using FA2-2 strains carrying the two plasmids as donor strains and JH2SS as the recipient strain. These results are representative of at least three independent experiments.
[c] These results are representative of at least three independent experiments.
[d] P1, P2, and P3 indicate the three potential promoter regions for *traB* as shown in Fig. 5 and Fig. S3 in the supplemental material.
[e] NT, not tested.
[f] The transformants showed poor growth.

firmed an operon structure composed of two genes as shown in Fig. 4, lanes 1 and 2.

Transcriptional analysis of ORF10 and ORF13 using Tn*917-lac* insertion mutants. *traB* encodes a 187-amino-acid protein and was necessary for both plasmid transfer and cell aggregation. The aggregation determinants and most of the transfer-related genes of pHTβ were located in the Tra I region, which was mapped to a point downstream of the Tra II region and about 19 kbp away from *traB* (see Fig. S1 in the supplemental material). This implied that *traB* might encode a positive regulator for the gene expression of the Tra I region. To examine whether *traB* regulates the gene expression of Tra I region, transcription analysis of the Tra I region was performed using Tn*917-lac* insertion mutants within the Tra I region. For this purpose, the two insertion mutants pHTβ::Tn*917-lac*/136 and pHTβ::Tn*917-lac*/154 were used for the construction of *traB* deletion derivatives (Fig. 2; Table 5) (32). The inserts in pHTβ::Tn*917-lac*/136 and pHTβ::Tn*917-lac*/154 were in the same orientation as that of the pHTβ plasmid ORFs and were mapped to ORF10 and ORF13, respectively, located in the aggregation region described above (32). Both of the mutants showed detectable *lacZ* activities, indicating that the expression of the aggregation determinants was constitutive (Table 5). These data were consistent with the data obtained from transcriptional analysis of the aggregation region in Tra I and the constitutive self-aggregation of strain FA2-2 carrying pHTβ. Each *traB* in-frame derivative mutant of pHTβ::Tn*917-lac*/136 and pHTβ::Tn*917-lac*/154 (pMG1008 and pMG1009) showed a decrease in transcript for ORF10 and ORF13, respectively. The reduction in transcription levels of

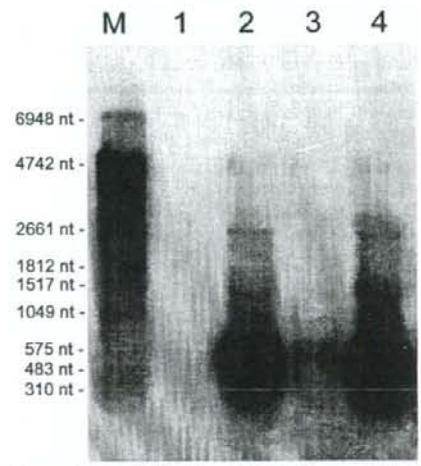

FIG. 6. Northern hybridization analysis of transcription of the aggregation determinant of pHTβ, ORF57 (*traA*), and ORF56 (*traB*) in-frame deletion mutants using ORF9 RNA probe. Two micrograms of total RNA was separated on an 0.8% agarose gel containing MOPS buffer and 2% formaldehyde. After the RNA was transferred onto a nylon membrane, the ORF9 RNA was detected by using the DIG-labeled ORF9 probe shown in Fig. 2C. The chemiluminescent substrate CDP-Star (Boehringer Mannheim) was used for visualization of the RNA bands. The positions of the DIG-labeled RNA molecular size marker I set (Boehringer Mannheim) are shown on the left. Lane M, RNA molecular size markers; lane 1, FA2-2; lane 2, FA2-2(pHTβ); lane 3, FA2-2(pMG1000 [ORF56 (*traB*) in-frame deletion mutant]); lane 4, FA2-2(pMG1001 [ORF57 (*traA*) in-frame deletion mutant]).

TABLE 5. Transcription activity of the aggregation region of pHTβ[a]

Resident plasmid (Tn*917-lac*-inserted ORF)	LacZ expression (MU) with complementary plasmid	
	pAM401 (vector)	pMG1007 (*traB*)
pHTβ::Tn*917-lac*/136 (ORF10)	75.6	NT[b]
pMG1008 (pHTβ::Tn*917-lac*/136 Δ*traB*) (ORF10)	3.4	86.1
pHTβ::Tn*917-lac*/154 (ORF13)	34.5	NT[b]
pMG1009 (pHTβ::Tn*917-lac*/154 Δ*traB*) (ORF13)	1.2	29.4

[a] These results are representative of at least three independent experiments.
[b] NT, not tested.

the ORFs was complemented in the mutants in *trans* by adding the *traB* plasmid clone to be equivalent to the levels of pHTβ::Tn*917-lac*/136 and/154 (Fig. 5) (Table 5). The results indicated that *traB* positively regulated the transcription (expression) of the aggregation determinants located in the Tra I region of pHTβ.

Northern hybridization analysis of the aggregation region of wild-type pHTβ and *traB* and *traA* mutants. The genetic analysis of the Tra II region showed that *traB* positively regulated the transcription of the aggregation region lying from ORF9 to ORF13 but *traA* did not. Northern hybridization analysis of each FA2-2 strain carrying wild-type pHTβ and in-frame deletion mutant of *traB* or *traA*, respectively, was performed using RNA probes for ORF9 and ORF13. Northern hybridization analysis using an ORF9 RNA probe detected a strong small transcript (around 600 nucleotides) in the wild-type pHTβ plasmid (Fig. 6, lane 2). A few bands were also detected in the strain carrying pHTβ, and the largest transcript was estimated as around 4,900 nucleotides in length. We could not detect any apparent band (transcripts) by Northern hybridization analysis using ORF13 RNA probe even if 10 micrograms of RNA was loaded on the gel (data not shown). Taking the gene organization of the aggregation region and RT-PCR results together, these data suggested the following. A large number of transcripts could be started from the strong promoter region upstream of ORF9 (i.e., P1, P2, and P3), and most of them ended at the terminator signal (inverted repeated sequences) located just upstream of ORF10 in the wild-type plasmid (Fig. 2C). A part of the transcripts from the promoter region could be transcribed beyond the terminator sequence to the downstream region of ORF10, ORF11, and ORF12 and ended at the next potential terminator sequence located between ORF12 and ORF13 (Fig. 2C). The transcript of ORF13 and its downstream region might be too long or too small in quantity to detect the product by Northern hybridization analysis in this study.

In strain FA2-2 carrying the *traB* in-frame deletion mutant plasmid, a weak transcript the same size as the small strong transcript detected in the wild-type plasmid was also detected (Fig. 6, lane 3). The transcript of ORF9 was significantly decreased, and the long transcripts were not detected in the mutant, suggesting that the promoter activity was strictly repressed and the transcript was terminated at the terminator signal upstream of ORF10.

The transcript profile of the *traA* mutant using ORF9 probe was almost identical to that of the wild-type plasmid (Fig. 6, lane 4). The results were consistent with the results from the genetic analyses described above.

Analysis of 71ORF2 (*traA*) and 71ORF1 (equivalent to *traB* of pHTβ) in-frame deletion mutants of pMG1. The genes equivalent to *traA* and *traB* were found in pMG1 (65.1 kb, Gm^r) and designated 71ORF2 and 71ORF1, respectively (26, 27, 32). The in-frame mutants of 71ORF2 and 71ORF1 of pMG1 were generated as described in Materials and Methods. In-frame deletion mutants of 71ORF2 (*traA*) and 71ORF1 (equivalent to *traB* of pHTβ) of pMG1 were designated pMG1101 and pMG1100, respectively, and both had in-frame deletions identical to pMG1001 (*traA* mutant of pHTβ) and pMG1000 (*traB* mutant of pHTβ), respectively. The macroscopic self-aggregations were not observed in FA2-2 strains carrying pMG1 and two mutants (Table 4). pMG1 transferred at the frequencies of 6.4×10^{-6} and 6.0×10^{-3} per donor cell in broth mating and solid surface mating, respectively (Table 4). pMG1100 (71ORF1 [*traB*] mutant of pMG1) transferred at a frequency of 4.6×10^{-7} and 3.3×10^{-4} per donor cell in broth mating and solid surface mating, respectively (Table 4). pMG1101 (71ORF2 [*traA*] mutant of pMG1) transferred at the same frequencies as those of pMG1 in broth mating and solid surface mating (Table 4). These results indicated that 71ORF1 (equivalent to *traB*) was associated with the efficient transfer of pMG1 in broth mating.

DISCUSSION

In this report, we have shown that the pHTβ plasmid confers the self-aggregation phenotype on the host *E. faecalis* strain and that the aggregation was positively controlled in *trans* by a newly identified *traB* gene. Self-aggregation of the donor strain was initiated by the formation of an aggregate between the donor and recipient strains during conjugation in liquid medium. The aggregation function was encoded on the pHTβ plasmid.

Cloning, deletion mutant, and insertion mutant analysis showed that the aggregation region was located in the upstream Tra I region, spanning a region of 6 kb lying between 5.6 kb and 11.6 kb of the pHTβ map and containing from the promoter region upstream of ORF9 to ORF13. In-frame deletion mutant analysis showed that ORF10 may be involved in the production of the AS, although the mutant showed a weak (reduced) aggregation phenotype. The AS protein of the pheromone-responsive plasmid pAD1 is organized in a domain structure, and it has been shown that the N-terminal region of the AS is responsible for aggregation (21). As the putative product of ORF10 shows no amino acid or DNA sequence homology with the pAD1 AS, we would need to carry out a detailed analysis of the ORF10 domain structure to show that ORF10 is the determinant for the AS. Analysis of the insertions into pHTβ suggested that the region downstream of ORF13 is associated with aggregation in the wild-type pHTβ plasmid but not involved specifically in aggregation for the plasmid transfer.

Of the potential promoters in this region, one (P3) of the

three promoters (P1 to P3) upstream of ORF9 showed strong promoter activity. The transcripts of each internal region between the ORFs from ORF9 to ORF14 were detected by RT-PCR analysis using the FA2-2 strain carrying pHTβ. Northern hybridization analysis of pHTβ using ORF9 probe showed a small transcript corresponding to the size of ORF9 and did not show a long transcript covering the ORF13 region and the transcript of ORF13. There is a possibility that most transcripts started from the promoter upstream of ORF9 and were terminated at a potential terminal signal located upstream of ORF13 and that a part of transcripts were elongated into the downstream region or that most transcript would be processed between ORF12 and ORF13. There is a possibility of a copy number effect produced by the multicopy vector plasmid in the efficient expression of the aggregation region.

The Tra II region consists of ORF56 (*traB*) and ORF57 (*traA*) (Fig. 5). Both *traA* and *traB* genes are specific for the pMG1-like plasmids, are conserved in all of the pMG-like plasmids examined (unpublished data), and are not found in other organisms. There were three potential promoter sequences (i.e., P1, P2, and P3) in front of the *traB* gene, and there was no good potential promoter sequence in the region just upstream of the *traA* gene (26). Genetic analysis of promoter activity showed that the promoter (P3) closest to *traB* might be a constitutive promoter for *traB* transcription. Although there is the possibility that the multicopy plasmid pAM401 may affect the efficient expression of the promoter, P3 initiated functional expression of *traB* in the cloned plasmid. RT-PCR analysis of pHTβ indicated that the *traA* and *traB* genes consist of an operon structure which is polycistronically transcribed from *traB* to *traA*.

Analysis of the in-frame deletion mutants of *traB*, *traB*/*traA*, and *traA* of pHTβ indicated that *traB* was necessary for plasmid transfer and the aggregation phenotype but that *traA* was not essential. The function of *traA* in pHTβ has not yet been elucidated. 71ORF1 and 71ORF2 (*traA*) of pMG1 are 100% and 98% homologous with the deduced amino acid sequences of *traB* and *traA* of pHTβ, respectively (26, 32). 71ORF2 (*traA*) is necessary for both the formation of the cell aggregate and the efficient transfer of pMG1, but the function of 71ORF1 has not yet been elucidated (26). 71ORF1 and 71ORF2 (*traA*) of pMG1 were aligned in this order and oriented in the same direction. In this study, analysis of each in-frame deletion mutant of 71ORF2 (*traA*) and 71ORF1 showed that 71ORF1 of pMG1 was associated with plasmid transfer but 71ORF2 (*traA*) was not related, a result which was inconsistent with a previous study (26). In the previous study of the function of *traA* of pMG1, the *traA*-disrupted mutant of pMG1 was constructed by cointegration of a suicide vector plasmid containing *traA* into the *traA* of pMG1 (26). In that study, the transcript initiated from the promoter of 71ORF1 (i.e., *traB*) stopped in the disrupted *traA* region and could not elongate beyond *traA*. A transcript reading from 71ORF1 of pMG1 or *traB* of pHTβ into the downstream region of Tra II might be necessary for full function of this region or for the stabilization of transcript.

The mode of positive regulation of *traB* has not yet been elucidated. An in-frame deletion mutant of *traB* of pHTβ resulted in defects in aggregation and transferability and was inhibited in the expression of transcript of the aggregation region. The *traB* in-frame deletion mutants of pHTβ::Tn*917-lac*/136 (i.e., pMG1008) and of pHTβ::Tn*917-lac*/154 (i.e., pMG1009), which were Tn*917-lac* insertion mutants in ORF10 and ORF13 of pHTβ, respectively, showed a greater reduction in *lacZ* expression than did their parent plasmids. Northern hybridization analysis of the aggregation region of the *traB* mutant of pHTβ also showed a reduced transcript which started from the upstream region of ORF9. The cloned *traB* complemented and restored the impaired *lacZ* expression of pMG1008 and pMG1009 to the levels found in the parent plasmids. These results indicated that *traB* positively regulated the expression of the aggregation region. On the other hand, clones within the aggregation region (i.e., pHT1010, pHT1011, pHT1012, and pHT1013) that did not carry *traB* showed the same aggregation phenotype as that of the wild-type plasmid in the host strain. The cloned promoter region for the aggregation-related Tra I region showed strong activity by itself in an FA2-2 background. These data implied that a negative regulator for aggregation might be encoded on the pHTβ plasmid and that the *traB* product could downregulate the negative regulator(s). The *traB* gene product might derepress the unidentified negative regulator for transfer-related genes and aggregation genes.

pMG1100, an in-frame deletion mutant of 71ORF1 of pMG1, still transferred in broth mating at a frequency of about 1/10 of that of the wild-type strain. Unlike the aggregation region of pHTβ, which was completely repressed in the pHTβ *traB* mutant, the result indicated that the transfer-related region of pMG1100, corresponding to the Tra I region of pHTβ, would not be completely repressed during the mating, implying that the mode of regulation would be different between pHTβ and pMG1.

The pheromone-responsive plasmids of *E. faecalis* are the best examples to be elucidated to date showing the mechanism of initial cell-to-cell contact in gram-positive bacteria. Cell-to-cell contact is mediated by donor and recipient aggregation, which results from donor cell aggregation induced by pheromone (4). In this study, we showed that a novel type of aggregation-mediated plasmid transfer system was present in enterococci. The donor strains carrying the pHTβ plasmid self-aggregated without recipient cells in broth culture, and this function is positively regulated in *trans*. Aggregation of the donor strains was associated with the efficient transfer of the pHTβ plasmid in the broth mating between donor and recipient cells, implying that the aggregation of donor cells precedes the formation of mating aggregates with recipient cells. The self-aggregation of the donor strain carrying the pHTβ plasmid implied that the plasmid transfer system was constitutively expressed.

ACKNOWLEDGMENTS

This work was supported by grants from the Japanese Ministry of Education, Culture, Sport, Science and Technology (Tokutei-ryoiki [Matrix of Infection Phenomena], Kiban [B], Kiban [C]) and the Japanese Ministry of Health, Labor and Welfare (H18-Shinko-11).

We thank Koichi Tanimoto and Shuhei Fujimoto for helpful advice. We thank Don B. Clewell for providing the plasmids used in this study. We also thank Elizabeth Kamei for revising the manuscript.

REFERENCES

1. **Abajy, M. Y., J. Kopec, K. Schiwon, M. Burzynski, M. Doring, C. Bohn, and E. Grohmann.** 2007. A type IV-secretion-like system is required for conjugative DNA transport of broad-host-range plasmid pIP501 in gram-positive bacteria. J. Bacteriol. **189**:2487–2496.

2. **Arthur, M., C. Molinas, F. Depardieu, and P. Courvalin.** 1993. Characterization of Tn*1546*, a Tn*3*-related transposon conferring glycopeptide resistance by synthesis of depsipeptide peptidoglycan precursors in *Enterococcus faecium* BM4147. J. Bacteriol. **175:**117–127.
3. **Clewell, D. B.** 1999. Sex pheromone systems in enterococci, p. 47–65. *In* G. M. Dunny and S. C. Winans (ed.), Cell-cell signaling in bacteria. ASM Press, Washington, DC.
4. **Clewell, D. B., and G. M. Dunny.** 2002. Conjugation and genetic exchange in enterococci, p. 265–300. *In* M. S. Gilmore, D. B. Clewell, P. Courvalin, G. M. Dunny, B. E. Murray, and L. B. Rice (ed.), The enterococci: pathogenesis, molecular biology, and antibiotic resistance. ASM Press, Washington, DC.
5. **Clewell, D. B., P. K. Tomich, M. C. Gawron-Burke, A. E. Franke, Y. Yagi, and F. A. An.** 1982. Mapping of *Streptococcus faecalis* plasmids pAD1 and pAD2 and studies relating to transposition of Tn*917*. J. Bacteriol. **152:**1220–1230.
6. **Dunny, G. M., B. L. Brown, and D. B. Clewell.** 1978. Induced cell aggregation and mating in *Streptococcus faecalis*: evidence for a bacterial sex pheromone. Proc. Natl. Acad. Sci. USA **75:**3479–3483.
7. **Dunny, G. M., and D. B. Clewell.** 1975. Transmissible toxin (hemolysin) plasmid in *Streptococcus faecalis* and its mobilization of a noninfectious drug resistance plasmid. J. Bacteriol. **124:**784–790.
8. **Dunny, G. M., L. N. Lee, and D. J. LeBlanc.** 1991. Improved electroporation and cloning vector system for gram-positive bacteria. Appl. Environ. Microbiol. **57:**1194–1201.
9. **Francia, M. V., A. Varsaki, M. P. Garcillan-Barcia, A. Latorre, C. Drainas, and F. de la Cruz.** 2004. A classification scheme for mobilization regions of bacterial plasmids. FEMS Microbiol. Rev. **28:**79–100.
10. **Franke, A. E., and D. B. Clewell.** 1981. Evidence for a chromosome-borne resistance transposon (Tn*916*) in *Streptococcus faecalis* that is capable of "conjugal" transfer in the absence of a conjugative plasmid. J. Bacteriol. **145:**494–502.
11. **Fujimoto, S., H. Hashimoto, and Y. Ike.** 1991. Low cost device for electrotransformation and its application to the highly efficient transformation of *Escherichia coli* and *Enterococcus faecalis*. Plasmid **26:**131–135.
12. **Fujimoto, S., and Y. Ike.** 2001. pAM401-based shuttle vectors that enable overexpression of promoterless genes and one-step purification of tag fusion proteins directly from *Enterococcus faecalis*. Appl. Environ. Microbiol. **67:**1262–1267.
13. **Fujimoto, S., H. Tomita, E. Wakamatsu, K. Tanimoto, and Y. Ike.** 1995. Physical mapping of the conjugative bacteriocin plasmid pPD1 of *Enterococcus faecalis* and identification of the determinant related to the pheromone response. J. Bacteriol. **177:**5574–5581.
14. **Grohmann, E., G. Muth, and M. Espinosa.** 2003. Conjugative plasmid transfer in gram-positive bacteria. Microbiol. Mol. Biol. Rev. **67:**277–301.
15. **Ike, Y., and D. B. Clewell.** 1984. Genetic analysis of the pAD1 pheromone response in *Streptococcus faecalis*, using transposon Tn*917* as an insertional mutagen. J. Bacteriol. **158:**777–783.
16. **Ike, Y., R. C. Craig, B. A. White, Y. Yagi, and D. B. Clewell.** 1983. Modification of *Streptococcus faecalis* sex pheromones after acquisition of plasmid DNA. Proc. Natl. Acad. Sci. USA **8:**5369–5373.
17. **Ike, Y., K. Tanimoto, H. Tomita, K. Takeuchi, and S. Fujimoto.** 1998. Efficient transfer of the pheromone-independent *Enterococcus faecium* plasmid pMG1 (Gm^r) (65.1 kilobases) to *Enterococcus* strains during broth mating. J. Bacteriol. **180:**4886–4892.
18. **LeBlanc, D. J., and L. N. Lee.** 1984. Physical and genetic analysis of streptococcal plasmid pAMβ1 and cloning of its replication region. J. Bacteriol. **157:**445–453.
19. **LeBlanc, D. J., L. N. Lee, and J. M. Inamine.** 1991. Cloning and nucleotide base sequence analysis of a spectinomycin adenyltransferase AAD(9) determinant from *Enterococcus faecalis*. Antimicrob. Agents Chemother. **35:**1804–1810.
20. **Miller, J. H.** 1972. Experiments in molecular genetics. Cold Spring Harbor Laboratory Press, Cold Spring Harbor, NY.
21. **Muscholl-Silberhorn, A.** 1998. Analysis of the clumping-mediating domain(s) of sex pheromone plasmid pAD1-encoded aggregation substance. Eur. J. Biochem. **258:**515–520.
22. **Perkins, J. B., and P. J. Youngman.** 1986. Construction and properties of Tn*917-lac*, a transposon derivative that mediates transcriptional gene fusions in *Bacillus subtilis*. Proc. Natl. Acad. Sci. USA **83:**140–144.
23. **Sambrook, J., E. F. Fritsch, and T. Maniatis.** 2001. Molecular cloning: a laboratory manual, 3rd ed. Cold Spring Harbor Laboratory Press, Cold Spring Harbor, NY.
24. **Schroder, G., and E. Lanka.** 2005. The mating pair formation system of conjugative plasmids—a versatile secretion machinery for transfer of proteins and DNA. Plasmid **54:**1–25.
25. **Tanimoto, K., and D. B. Clewell.** 1993. Regulation of the pAD1-encoded sex pheromone response in *Enterococcus faecalis*: expression of the positive regulator TraE1. J. Bacteriol. **175:**1008–1018.
26. **Tanimoto, K., and Y. Ike.** 2002. Analysis of the conjugal transfer system of the pheromone-independent highly transferable *Enterococcus* plasmid pMG1: identification of *tra* gene (*traA*) up-regulated during conjugation. J. Bacteriol. **184:**5800–5804.
27. **Tanimoto, K., and Y. Ike.** 15 September 2008. Complete nucleotide sequencing and analysis of the 65-kb highly-conjugative *Enterococcus faecium* plasmid pMG1: identification of the transfer-related region and the minimum region required for replication. FEMS Microbiol. Lett. **288:**186–195.
28. **Tomich, P. K., F. Y. An, and D. B. Clewell.** 1980. Properties of erythromycin-inducible transposon Tn*917* in *Streptococcus faecalis*. J. Bacteriol. **141:**1366–1374.
29. **Tomita, H., and D. B. Clewell.** 2000. A pAD1-encoded small RNA molecule, mD, negatively regulates *Enterococcus faecalis* pheromone response by enhancing transcription termination. J. Bacteriol. **182:**1062–1073.
30. **Tomita, H., S. Fujimoto, K. Tanimoto, and Y. Ike.** 1996. Cloning and genetic organization of the bacteriocin 31 determinant encoded on the *Enterococcus faecalis* pheromone-responsive conjugative plasmid pYI17. J. Bacteriol. **178:**3585–3593.
31. **Tomita, H., S. Fujimoto, K. Tanimoto, and Y. Ike.** 1997. Cloning and genetic and sequence analyses of the bacteriocin 21 determinant encoded on the *Enterococcus faecalis* pheromone-responsive conjugative plasmid pPD1. J. Bacteriol. **179:**7843–7855.
32. **Tomita, H., and Y. Ike.** 2005. Genetic analysis of transfer-related regions of the vancomycin resistance *Enterococcus* conjugative plasmid pHTβ: identification of *oriT* and a putative relaxase gene. J. Bacteriol. **187:**7727–7737.
33. **Tomita, H., C. Pierson, S. K. Lim, D. B. Clewell, and Y. Ike.** 2002. Possible connection between a widely disseminated conjugative gentamicin resistance (pMG1-like) plasmid and the emergence of vancomycin resistance in *Enterococcus faecium*. J. Clin. Microbiol. **40:**3326–3333.
34. **Tomita, H., K. Tanimoto, S. Hayakawa, K. Morinaga, K. Ezaki, H. Oshima, and Y. Ike.** 2003. Highly conjugative pMG1-like plasmids carrying Tn*1546*-like transposons that encode vancomycin resistance in *Enterococcus faecium*. J. Bacteriol. **185:**7024–7028.
35. **Weaver, K. E., and D. B. Clewell.** 1988. Regulation of the pAD1 sex pheromone response in *Enterococcus faecalis*: construction and characterization of *lacZ* transcriptional fusions in a key control region of the plasmid. J. Bacteriol. **170:**4343–4352.
36. **Weaver, K. E., and D. B. Clewell.** 1990. Regulation of the pAD1 sex pheromone response in *Enterococcus faecalis*: effects of host strain and *traA*, *traB*, and C region mutants on expression of an E region pheromone-inducible *lacZ* fusion. J. Bacteriol. **172:**2633–2641.
37. **Weaver, K. E., and S. G. Reddy.** 2006. The recombination deficient *Enterococcus faecalis* UV202 strain is a *recA* mutant. Plasmid **55:**164–168.
38. **Wirth, R., F. Y. An, and D. B. Clewell.** 1986. Highly efficient protoplast transformation system for *Streptococcus faecalis* and a new *Escherichia coli-S. faecalis* shuttle vector. J. Bacteriol. **165:**831–836.
39. **Yagi, Y., and D. B. Clewell.** 1980. Recombination-deficient mutant of *Streptococcus faecalis*. J. Bacteriol. **143:**966–970.
40. **Zechner, E. L., F. de la Cruz, R. Eisenbrandt, A. M. Grahn, G. Koraimann, E. Lanka, G. Muth, W. Pansegrau, C. M. Thomas, B. M. Wilkins, and M. Zatyka.** 2000. Conjugative-DNA transfer processes, p. 87–174. *In* C. M. Thomas (ed.), The horizontal gene pool. Bacterial plasmids and gene spread. Harwood Academic Publishers, Amsterdam, The Netherlands.

ANTIMICROBIAL AGENTS AND CHEMOTHERAPY, Oct. 2008, p. 3795–3800 Vol. 52, No. 10
0066-4804/08/$08.00+0 doi:10.1128/AAC.00464-08

Fluoroquinolone Enhances the Mutation Frequency for Meropenem-Selected Carbapenem Resistance in *Pseudomonas aeruginosa*, but Use of the High-Potency Drug Doripenem Inhibits Mutant Formation▽

Koichi Tanimoto,[2] Haruyoshi Tomita,[1] Shuhei Fujimoto,[1] Katsuko Okuzumi,[3] and Yasuyoshi Ike[1,2]*

Department of Bacteriology[1] and Laboratory of Bacterial Drug Resistance,[2] Gunma University Graduate School of Medicine, Maebashi, Gunma 371-8511, Japan, and Department of Medical Safety Administration Division of Infection Control, Dokkyo Medical University Hospital, Shimotsuga, Tochigi 321-0293, Japan[3]

Received 8 April 2008/Returned for modification 22 May 2008/Accepted 4 August 2008

The mutation frequency for carbapenem resistance in *Pseudomonas aeruginosa* strains that were selected with carbapenems was enhanced in the presence of subinhibitory concentrations of fluoroquinolones. The mutants showed either a loss of OprD activity or increased *mexAB-oprM* expression. The highest mutant isolation frequency was obtained by selection with meropenem, while doripenem inhibited mutant growth.

The carbapenem group of β-lactam antibiotics is highly active against *Pseudomonas aeruginosa*. In the absence of the carbapenem-hydrolyzing enzyme metallo-β-lactamase, carbapenem resistance mechanisms include reduced expression of OprD (3, 24, 32, 33) and increased expression of *mexAB-oprM* (6, 11, 13, 17, 23) or AmpC cephalosporinase (14, 15, 23). The interplay between AmpC cephalosporinase and the loss of OprD is an essential element of carbapenem resistance (14). The reduction in OprD expression found in *P. aeruginosa* is the result of a spontaneous mutation lacking the D2 (OprD) porin outer membrane protein (3, 24, 32, 33). The isolation frequency of carbapenem resistance in *P. aeruginosa* clinical iso-

TABLE 1. Drug susceptibilities and genotypes of the *P. aeruginosa* strains and its derivatives in this study

Strain[a]	Genotype or phenotype	MIC (μg/ml)[b]							
		DRPM	MEPM	IPM	CAZ	PIPC	GM	CPFX	OFLX
PAO1	Parent	0.2	0.2	0.8	1.6	3.1	1.6	0.2	0.8
PAO1KTL	*oprD*	0.8	1.6	12.5	1.6	3.1	1.6	0.2	0.8
PAO1KTL1	*oprD mexAB*(Hy)-*oprM*(Hy)	1.6	6.3	12.5	6.3	12.5	1.6	0.8	3.1
PAO1KTS	*mexAB*(Hy)-*oprM*(Hy)	0.4	1.6	0.8	6.3	12.5	1.6	0.8	3.1
PAO1IPM46	*oprD*	0.8	1.6	12.5	1.6	3.1	1.6	0.2	0.8
PAO1SO20	*mexAB*(Hy)-*oprM*(Hy)	0.4	1.6	0.8	6.3	12.5	1.6	0.8	3.1
GP4	Wild type	0.2	0.2	0.8	1.6	100	100	0.2	1.6
GP4KT11	*oprD*	1.6	3.1	12.5	1.6	100	100	0.2	1.6
GP4KT111	*oprD mexAB*(Hy)-*oprM*(Hy)	3.1	12.5	12.5	6.3	200	100	0.8	6.3
GP20	Wild type	0.2	0.2	0.8	1.6	100	3.1	0.2	1.6
GP20KT21	*oprD*	1.6	3.1	12.5	1.6	100	3.1	0.2	1.6
GP37	Wild type	0.2	0.2	0.8	1.6	100	100	0.2	1.6
GP37KT31	*oprD*	1.6	3.1	12.5	1.6	100	100	0.2	1.6
GP62	Wild type	0.1	0.2	0.8	1.6	100	1.6	0.2	1.6
GP62KT41	*oprD*	0.8	3.1	12.5	1.6	100	1.6	0.2	1.6
GP61	Wild type, *oprD*	0.8	1.6	6.3	3.1	3.1	1.6	0.2	1.6
GP61KT51	*oprD mexAB*(Hy)-*oprM*(Hy)	1.6	6.3	6.3	12.5	12.5	1.6	0.8	6.3

[a] PAO1IPM46 and PAO1SO20 are reported PAO1 mutants with decreased *oprD* expression and increased *mexAB-oprM* expression, respectively (18). *P. aeruginosa* GP4, GP20, GP37, and GP62 are carbapenem-susceptible clinical isolates. The clinical strain GP61 was used as the representative wild-type strain with a higher imipenem MIC. The reduced expression of *oprD* in GP61 is shown in Fig. 1. During this study, the drug susceptibilities of the mutant strains isolated on the agar plates containing the selective carbapenem drugs DRPM, MEPM, and IPM, respectively, were examined and representative strains are shown. The representative mutant strains PAO1KTL and PAO1KTS were isolated from PAO1, and GP4KT11, GP20KT21, GP37KT31, and GP62KT41 were isolated from GP4, GP20, GP37, and GP62, respectively. The representative mutant strains PAO1KTL1, GP4KT111, and GP61KT51 were isolated from the *oprD* mutants of PAO1KTL, GP4KT11, and clinical isolate GP61, respectively.

[b] DRPM is a new carbapenem that has been developed by Shionogi Pharmaceuticals, Osaka, Japan) (7, 8, 19). Abbreviations for the other antibiotics used are as follows: CAZ, ceftazidime; PIPC, piperacillin; GM, gentamicin; CPFX, ciprofloxacin; and OFLX, ofloxacin.

* Corresponding author. Mailing address: Department of Bacteriology, Gunma University Graduate Schooi of Medicine, 3-39-22 Showa-Machi, Maebashi, Gunma 371-8511, Japan. Phone: 81-27-220-7990. Fax: 81-27-220-7996. E-mail: yasuike@med.gunma-u.ac.jp.

▽ Published ahead of print on 11 August 2008.